FEATHER RIVER HYDROLOGIC OBSERVATORY: IMPROVING SNOWPACK FORECASTING FOR HYDROPOWER GENERATION USING INTELLIGENT INFORMATION SYSTEMS

A Report for:

California's Fourth Climate Change Assessment

Prepared By:
Francesco Avanzi[1], Tessa P. Maurer[1], Sami A. Malek[1], Prof. Steven D. Glaser (PI)[1], Prof Roger C. Bales (co-PI)[1,2], Prof Martha H. Conklin (co-PI)[2]

[1]University of California, Berkeley
[2]University of California, Merced

Edmund G. Brown Jr., *Governor*

August 2018
CCCA4-CEC-2018-001

ACKNOWLEDGEMENTS

This work was supported by the California Energy Commission through the grant "Improving Hydrological Snowpack Forecasting for Hydropower Generation Using Intelligent Information Systems" (EPC-14-067), Pacific Gas and Electric Co, the California Department of Water Resources, UC Water, Inria through the REALMS associate team, and the European Commission through the H2020 F-Interop and H2020 ARMOUR projects.

We thank Guido Franco, Susan Fischer Wilhelm, and Katharina Snyder (California Energy Commission); Boone Lek and David Rizzardo (Department of Water Resources); Kevin Richards, Gary Freeman, Matt Meadows, and Teri Smyly (PG&E); Peter Hartsough (University of California, Davis); and Thomas Watteyne and Keoma Brun-Laguna (Inria) for their guidance and support throughout the design of networks and the work with the PRMS model. We also would like to thank those who participated in the network deployment. They include Zeshi Zheng, Amanda Lee, Robert Taylor, Ansel Mcclelland, Katya Rakhmatulina, Wassim Lababidi, Mohammad Tuqan, and Ziran Zhang (UC Berkeley and UC Davis). We also thank Carlos A. Oroza (UC Berkeley), who supported us with the identification of measurement locations at each wireless sensor network site.

Comparative results using wireless sensor network data from the American and Kings River were partially supported by the National Science Foundation (EAR-1126887), the Southern Sierra Critical Zone Observatory (EAR-0725097), the California Department of Water Resources, and USDA-ARS CRIS Snow and Hydrologic Processes in the Intermountain West (American River), the Southern Sierra Critical Zone Observatory and the US Forest Service, USFS Pacific Southwest Research Station (Kings River Experimental Watersheds, Kings River). Tessa Maurer was supported by the National Science Foundation Graduate Research Fellowship under Grant No. DGE 1106400. We thank Zeshi Zheng (UC Berkeley), Mohammad Safeeq, Xiande Meng, and Robert Rice (UC Merced) for their invaluable assistance with input data. Francesco Avanzi is grateful to Nander Wever, Mathias Bavay (WSL SLF, Switzerland), and Isabelle Gouttevin (IRSTEA, France) for their support with SNOWPACK simulations.

California satellite map from the USGS National Map Small-Scale Collection. Ground-based data of SWE and precipitation were obtained from the California Data Exchange Center (CDEC, see http://cdec.water.ca.gov/).

PREFACE

California's Climate Change Assessments provide a scientific foundation for understanding climate-related vulnerability at the local scale and informing resilience actions. These Assessments contribute to the advancement of science-based policies, plans, and programs to promote effective climate leadership in California. In 2006, California released its First Climate Change Assessment, which shed light on the impacts of climate change on specific sectors in California and was instrumental in supporting the passage of the landmark legislation Assembly Bill 32, California's Global Warming Solutions Act. The Second Assessment concluded that adaptation is a crucial complement to reducing greenhouse gas emissions (2009), given that some changes to the climate are ongoing and inevitable, motivating and informing California's first Climate Adaptation Strategy released the same year. In 2012, California's Third Climate Change Assessment made substantial progress in projecting local impacts of climate change, investigating consequences to human and natural systems, and exploring barriers to adaptation.

Under the leadership of Governor Edmund G. Brown, Jr., a trio of state agencies jointly managed and supported California's Fourth Climate Change Assessment: California's Natural Resources Agency (CNRA), the Governor's Office of Planning and Research (OPR), and the California Energy Commission (Energy Commission). The Climate Action Team Research Working Group, through which more than 20 state agencies coordinate climate-related research, served as the Steering Committee, providing input for a multi-sector call for proposals, participating in selection of research teams, and offering technical guidance throughout the process.

California's Fourth Climate Change Assessment (Fourth Assessment) advances actionable science that serves the growing needs of state and local-level decision-makers from a variety of sectors. It includes research to develop rigorous, comprehensive climate change scenarios at a scale suitable for illuminating regional vulnerabilities and localized adaptation strategies in California; datasets and tools that improve integration of observed and projected knowledge about climate change into decision-making; and recommendations and information to directly inform vulnerability assessments and adaptation strategies for California's energy sector, water resources and management, oceans and coasts, forests, wildfires, agriculture, biodiversity and habitat, and public health.

The Fourth Assessment includes 44 technical reports to advance the scientific foundation for understanding climate-related risks and resilience options, nine regional reports plus an oceans and coast report to outline climate risks and adaptation options, reports on tribal and indigenous issues as well as climate justice, and a comprehensive statewide summary report. All research contributing to the Fourth Assessment was peer-reviewed to ensure scientific rigor and relevance to practitioners and stakeholders.

For the full suite of Fourth Assessment research products, please visit www.climateassessment.ca.gov. This report contributes to energy sector resilience by providing methods to improve management of hydropower through improved streamflow forecasting.

ABSTRACT

Changing climatic conditions and a lack of representative snow cover data challenge the ability to accurately model and fully utilize the water resources of montane snowpack on which California depends. This project aims to improve scientific understanding of snowpack modeling and streamflow forecasting techniques. Though relevant across industries and the state, this research focuses on hydropower applications in the North Fork of the Feather River. Central components of the project are four wireless sensor networks, installed in locations that are representative of vegetation and topography patterns across the basin. The networks collect snow, temperature, relative humidity, soil moisture, and soil temperature data every 15 minutes. By blending this information with remote sensing data and historical maps, we estimate the spatial distribution of snow water resources at high resolution. These outputs can help improve runoff forecasting tools such as the Precipitation-Runoff Modeling System (PRMS). Preliminary results show that wireless sensor networks can successfully track hydrologic states and fluxes in real time and provide a more representative picture of snowpack accumulation and melt than traditional index stations. Network data are also used to gain insight into rain-on-snow events, which are a key streamflow generation mechanism for the Feather River. The data show that the current calibration of PRMS on the Feather River could overestimate snowfall and underestimate liquid precipitation. Future steps include a sensitivity analysis of PRMS to identify its dominant parameters and conceptual limitations, as well as a full, dynamic recalibration of the model. Blended maps of snow water equivalent will also be assimilated into the model. These results will be included in the decision-support suite for PG&E, California's largest electric and natural gas utility, and an analysis will be performed to assess results' economic value for stakeholders in the energy and water-supply sectors.

Keywords: wireless sensor networks, hydrologic forecasting, hydropower, climate change, PRMS model, snow water equivalent, snow melt runoff, streamflow, remote sensing

Please use the following citation for this paper:

Avanzi, Francesco, Tessa Maurer, Sami Malek, Steven D. Glaser, Roger C. Bales, Martha H. Conklin. (UC Berkeley and UC Merced). 2018. ***Feather River Hydrologic Observatory: Improving Hydrological Snowpack Forecasting for Hydropower Generation Using Intelligent Information Systems.*** California's Fourth Climate Change Assessment, California Energy Commission. Publication Number: CNRA-CEC-2018-001.

HIGHLIGHTS

- This research demonstrates the use of wireless sensor networks in tracking hydrologic states and fluxes, which are key to understanding storage and release of water from California's snowpack, across physiographically representative locations, as well as their resilience to extreme snow conditions.
- Networks show capability of detecting and quantifying key streamflow generation mechanisms in real time. Examples include infiltration of water in soils during rain-on-snow events and transitions between periods dominated by either snow melt or evapotranspiration.
- Data from these networks can be blended with traditional sensors to enhance existing weather and snowpack-monitoring capabilities on the Feather River. For example, snow-depth data from wireless sensor networks can be combined with traditional devices for measuring snowpack (snow pillows) and precipitation gauges to improve phase (rain or snow) identification methods.
- Areas prone to rain-on-snow events, such as the Feather River basin, have been among the first to see the effects of increasing global temperatures.
- Networks can support better energy- and mass-balance models by improving data inputs and parameter calibration. Opportunities include combining data from wireless sensor networks with remote sensing to perform multi-objective calibration of hydrologic models and data assimilation.
- The ongoing work aims to improve forecasting of streamflow and thus quantify benefits of this decision-support system for electric utilities and other stakeholders on the Feather River, such as water agencies.
- An important goal of the project is to estimate changes in generation economics using wireless sensor networks as measurement tools. Doing so requires full cooperation of PG&E, which is expected. A paper on this topic will be submitted by August 2019.

WEB LINKS

http://frho.us/

TABLE OF CONTENTS

1: Introduction

1.1 Context: California's Water and Energy in a Changing Climate

California, like most parts of the world, is facing growing pressure on its human and natural systems from climate change [13, 28]. Warming temperatures are projected to increase the length and severity of droughts and contribute to more serious heat waves and wildfires [16]. These issues are likely to be particularly problematic for the state's water supply system [55].

California has one of the most intricate and complex water delivery systems in the world, with a network of reservoirs, aqueducts, and groundwater pumps that deliver water from the headwaters in the northern and eastern portions of the state to population centers and agricultural land in the west and south. The two primary delivery systems, the Central Valley Project and the State Water Project, deliver water over distances of 500 and 600 miles, respectively (800 and 960 km) [50, 73]. In addition to balancing the need for human drinking water and irrigation supply, various environmental considerations are enshrined in state law. These require, for example, that minimum flows are maintained in certain water ways for the benefit of native aquatic species.

Water in California is also intertwined with energy production; in 2016, hydroelectricity accounted for nearly 15% of in-state electricity generation [12]. Other energy sources such as natural gas plants rely on water for cooling. Conversely, water-related energy consumption accounts for 19% of the state's electricity and 30% of its natural gas consumption. Temperature increases [79] can lead to reduced water supply and water stress [81]. In response to these effects, the state is also starting to use more energy-intensive water supplies, such as desalinated water and deeper groundwater, which requires more energy consumption to pump to the surface [30].

Currently, California's system relies on fairly rigid expectations of seasonal and interannual water availability, as well as location and type of precipitation. A geographic imbalance between water supply and water demand, coupled with minimal storage near end users, means that the system lacks long-term resilience to drought and is not able to fully capture and store all available water in wet years [24]. Significant changes to the amount, timing, or quality of available water will strain this already sensitive balance. Many of the other impacts of climate change will exacerbate the problems; warmer temperatures will likely spur higher water use among the state's population. Longer droughts will necessitate a more flexible water storage system to maintain reserves for dry years. However, the extreme weather exacerbated by climate change may also mean that wet years become, on average, wetter. Such a situation could raise the risk of flooding and damage water infrastructure such as dams and water distribution systems [24].

Climate change may also contribute to water quality degradation in several ways. Warmer temperatures will lead to warmer water, which could have an adverse effect on native fish populations such as salmon [42]. Energy resources that rely on

water for cooling may see degraded efficiencies with warmer water temperatures [53]. If wildfire activity and severity increase [76, 77, 78], surrounding waterways will become more susceptible to contamination by toxic ash and debris [48, 59]. Expanding use of desalination will generate increasing amounts of highly saline brine, which can substantially harm water quality if not disposed of properly [24].

The following report focuses on the climate change impacts on the state's snowpack, an integral component of its water and energy system [5]. It describes how specific research efforts aim to improve understanding and estimation of snowpack conditions, particularly under shifting hydrologic regimes due to climate-change context [41].

1.2 Focus: California Snow Hydrology and Climate Change

The state of California relies heavily on winter snowfall for its annual water supply; melting snowpack from mountains in the northern and eastern regions of the state accounts for more than 60% of the state's consumptive water and up to one-third of total supply [11, 49]. Falling primarily between the months of November and April, the snowpack traditionally serves as a low-cost water storage option. As the snow melts through the spring and dry summer, the runoff that is generated is incrementally captured by the state's numerous water storage reservoirs. From there, it is released as needed to downstream communities for drinking and irrigation water. Streams and rivers fed by snowpack are also an important source of hydroelectricity production [65].

In general, the state's reservoirs are sized to accept water over an extended period, relying on the snowpack to mitigate the inflow of winter precipitation. Though reservoirs are legally obligated to maintain some storage space for emergency flood scenarios, their capacity for handling greatly increased inflows is limited. While climate change projections for California are divided on how the overall quantity of precipitation will be affected, warming temperatures will cause more of the precipitation to fall as rain rather than snow [40]. The reduction in snowpack will test the state's existing water storage capacity, increasing the potential for flood events and potentially reducing water agencies' abilities to maintain buffering supplies, both seasonally and year to year [54].

These changes will result in the rain/snow transition zone rising in elevation, so that mid-elevation locations that currently experience mixed or primarily snow events will receive more rain [25]. Warming temperatures will also lengthen the growing season for alpine vegetation, increasing evapotranspiration [22, 33]. Net runoff is therefore expected to decrease [8].

The magnitudes of these combined effects are challenging to anticipate, but there is substantial evidence that adaption will be costly [24]. The storage services currently provided by the snowpack, for example, will need to be replaced with another part of the state's water infrastructure system. Otherwise, a shift in streamflow seasonality could translate into a net loss of water available for civil, industrial, and agricultural uses [54]. A reduction in overall available water has the potential to significantly impact the state's precarious water balance, especially as the population grows. Understanding the mechanisms and impacts of the changing

climate will be imperative for the future management of California's water and hydroelectricity supplies.

1.3 Hydropower and Climate Change

Hydroelectric plants tend to have lower climate change impacts than fossil fuel energy sources such as natural gas and coal. As such, these plants are important to maintain as a component in energy portfolios. For example, the largest energy utility in Northern California, Pacific Gas & Electric (PG&E, see https://www.pge.com/), maintains hydropower plants on rivers across the Sierra Nevada, which runs along the eastern edge of the state from the Feather River basin north of Sacramento to the Kern River basin east of Bakersfield. In total, the utility's hydroelectricity-power capacity is 3,900 MW [66]. However, the future productivity and economic viability of hydropower facilities are threatened by changes in climate and energy portfolios.

More variable and extreme weather could undermine traditional forecasting methods, in which stream flow is generally predicted by regressing against historical patterns of snow melt and runoff [47]. Forecasting uncertainty is exacerbated by the frequent lack of representative measurement sites at high elevation, where most of snow accumulates and contributes to stream flow during summer [62] A good example of this data gap is the heat wave in June 2017, which caused massive snow melt at high elevation in the Kings River basin that could not be monitored in real time [67]. This growing uncertainty in runoff makes day-to-day operations of hydropower plants more uncertain, necessitating accurate daily streamflow estimates.

Accurate streamflow forecasts are even more important as a result of the 2015 passage of California's Senate Bill 350, which mandates that California's utility companies increase the proportion of renewable energy in their portfolios to 50% by 2050 [43]. The inclusion of often-intermittent renewable energy sources, like solar and wind power, has made energy pricing less predictable. At any given moment, excess wind and solar resources flooding the electricity grid may drive prices negative. This causes a situation in which any additional energy resources supplying the grid (including hydropower) will cost rather than produce profit for the utility company [29, 56]. The uncertainty in electricity prices coupled with uncertainty in stream flow forecasts can render hydropower plants uneconomical for utility companies [56]. It is beneficial to both utility companies and the California public to improve forecasting models and maintain the economic viability of these energy sources.

2: Scope of Work

This project aims to improve hydrologic snow-melt and streamflow forecasting using intelligent information. The final goal is to develop the core elements of a next-generation hydrographic data network and use this newly gained information to provide more adaptive decision-support tools for water resources forecasting. By including state agencies and stakeholders like PG&E, the project is expected to help

offset growing uncertainty in hydropower and water forecasting owing to growing demand, an increasingly variable energy portfolio, and a changing climate. More accurate forecasts will reduce the risk and associated costs assumed by PG&E and other stakeholders, and by extension, the California rate- and tax-payers.

2.1 Study Area

We focus primarily on the North and Middle Fork of the Feather River (FR, Figure 1). The river is in northern California at the conjunction between the Sierra Nevada and the Cascade mountain ranges. The Feather River is an important tributary of the Sacramento River, draining an area of about 6,000 mi^2 (15,500 km^2). Approximately half of that area (3,600 mi^2, or 9,400 km^2) drains into Lake Oroville, the largest reservoir of the State Water Project. Water from the Feather River constitutes about a third of all water distributed by the Metropolitan Water District of Southern California, the wholesale water retailer serving Los Angeles, San Diego, and the South Coast.

2.1.1 North Fork

The North Fork of the Feather River has headwaters in the northern portion of the catchment near Lassen Peak. A major tributary, the East Branch, meets the North Fork near Belden. Upstream of this confluence, the Upper North Fork Feather River Project by PG&E comprises three reservoirs and five powerhouses. The most important reservoir is Lake Almanor, a natural, largely spring-fed lake that was augmented by the construction of Canyon Dam. The other two reservoirs are Butt Valley, located on Butt Creek, and Belden Forebay. Lake Almanor, Butt Valley, and Belden Forebay have a total gross capacity of about 1,100,000 AF, 50,000 AF, and 2,400 AF, respectively (1.36×10^9 m^3, 6.17×10^7 m^3, and 3×10^6 m^3). These three reservoirs are interconnected through a complex network of tunnels and penstocks as shown in Figure 2. The five powerhouses are Hamilton Branch, Butt Valley, Caribou (1 and 2), Belden, and Oak Flat. Overall, the nominal capacity is 367 MW. A specific branch of North Fork of the Feather River includes Mt. Meadows reservoir and the Hamilton Branch powerhouse [31].

The East Branch of the North Fork (EBNF) encompasses some 1,025 mi^2 (2,655 km^2) and is less developed for hydropower than the main stem of the North Fork [21]. Sparse data for the East Branch make the unregulated flows particularly uncertain to model. Minimum daily temperatures, especially in the summer, have risen significantly during the past 35 years [21]. As a result, annual water-year outflow of the subbasin has started decreasing since about the 1960s [21]. This trend has resulted in a negative impact on PG&E's hydroelectric production through both direct equivalent energy losses as well as a rise in the uncertainty about the amount of snowpack storage.

The most relevant subbasins of the East Branch are Spanish Creek and Indian Creek. Indian Creek originates in the northern part of the basin and flows through Indian Valley close to Greenville, Crescent Mills, and Taylorsville. Spanish Creek is more southerly and crosses the American Valley close to Quincy, one of the largest towns in the basin. The main land use here is agricultural. The confluence between the East Branch and the North Fork is

located at Belden, from which point flows from the East Branch can substantially impact downstream operations.

Indeed, optimizing water planning for Lake Almanor is highly dependent on understanding the uncontrolled flows from the East Branch. The ridge between the East Branch and the North Fork represents an important rain shadow for moist air moving east from the Pacific Ocean [21].

Between the Middle and North Forks is Bucks Lake reservoir, managed by PG&E and directly connected to the Grizzly and Bucks Creek powerhouses and Grizzly Forebay (again, see Figure 2). Water from Bucks Lake ultimately drains into the North Fork and then Lake Oroville.

While the West Branch is now a direct tributary of Lake Oroville, this tributary was originally a branch of the North Fork (hence the name).

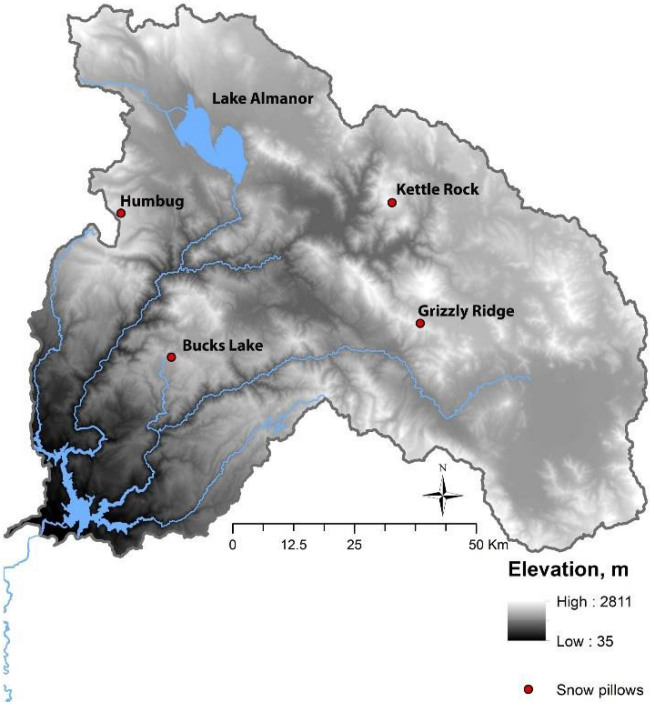

Figure 1: Map of the Feather River above the Thermalito Afterbay of the Oroville – Thermalito complex. Red dots represent the site of the four target sites where wireless sensor networks have been deployed (see Section 3.1.2). 12.5, 25, and 50 km correspond to 7.7, 15.5, and 31 miles, respectively.

2.1.2 Middle and South Forks

The Middle Fork of the Feather River (MFFR) is of comparable length to the North Fork (about 100 miles and 70 miles, or 160 and 112 km, respectively). The headwaters are located at the north- eastern boundary of the Feather River basin (Sierra Valley), where water from Lake Davis and several minor streams flows into one another. The total area of the Middle Fork is 1,046 mi^2, or 2,706 km^2.

The South Fork is of considerably smaller extent compared to both the North Fork and the Middle Fork (107 mi^2, or 278 km^2), but drains some relevant reservoirs like the Little Grass Valley Reservoir. Further details can be found in [31].

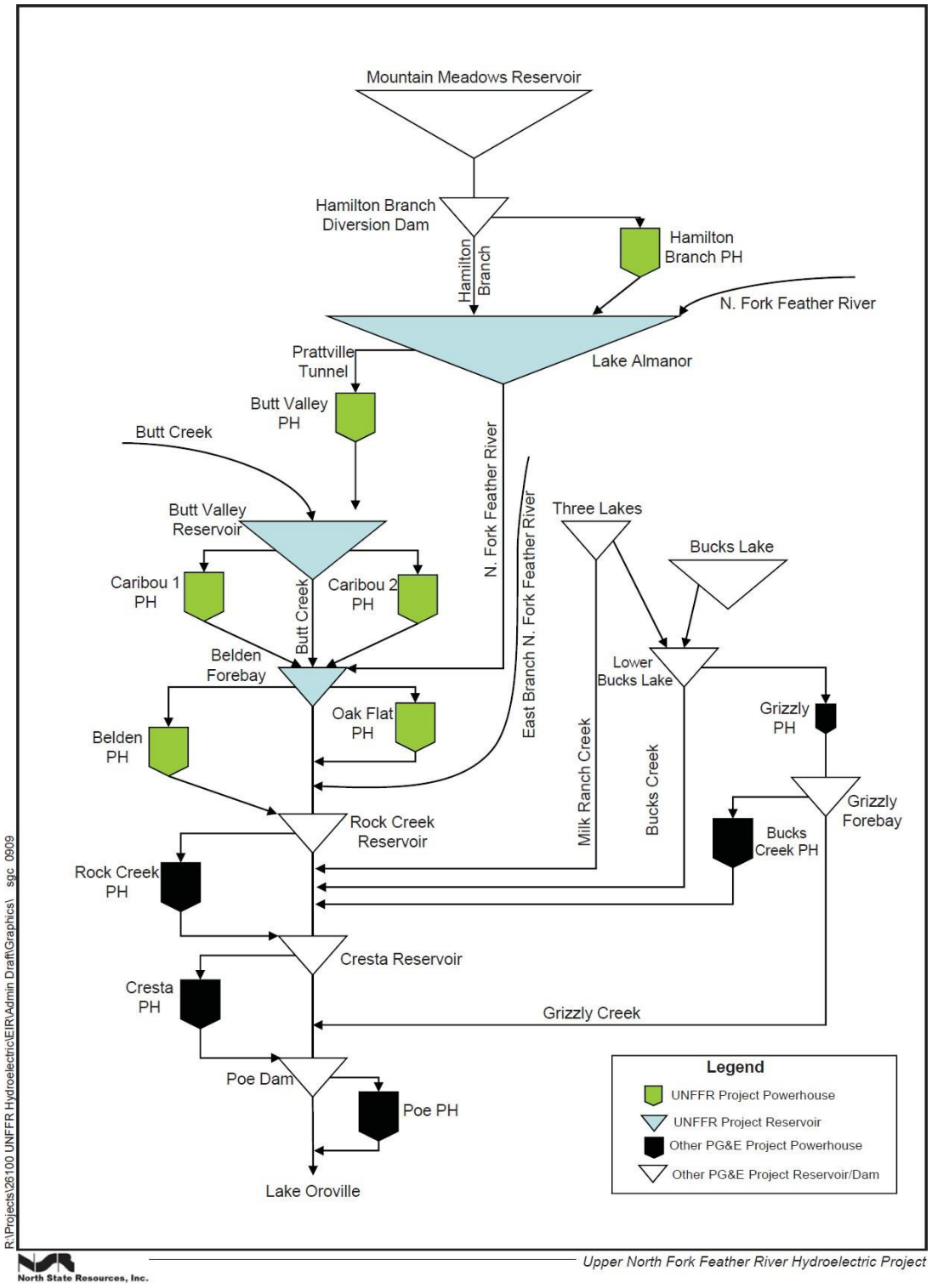

Figure 2: Schematic of the Upper North Fork Feather River Project and other PG&E projects on the river (source: [71]).

2.2 Hydrology of the Feather River

The Feather River basin is a hydrologically unique watershed. Straddling the border between the southern Cascades and the northern Sierra Nevada, the basin's geology varies from more permeable volcanic soil in the northern and western portions of the basin to harder, granitic soils in the southern portion [31]. The basin is the only watershed in the Sierra Nevada in which water east of the Sierra Divide cuts through the crest and drains to the west. The portion that drains into Lake Oroville has a lower average elevation than other Sierra watersheds, with a peak elevation of about 10,440 ft (3,182 m) at Lassen Peak [72]. The lower elevations make the basin more prone to mixed rain-snow events as well as rain-on-snow events in the wintertime [31], both of which are notoriously challenging to model [60]. Areas that are prone to rain-on-snow events, like the Feather, have been among the first to see the effects of increasing global temperatures.

Water year (WY) 2017 was particularly demonstrative of the impacts of severe rain-on-snow events. Between December 2016 and March 2017, periodic and intense atmospheric rivers from the Pacific Ocean hit the Californian coast. These storms resulted in significant reservoir management challenges due to the substantial influxes of water to Lake Oroville after each event. The most consequential storm of the season occurred in February. The simultaneous damage of the Oroville Dam spillway caused the California Department of Water Resources (DWR) to operate the emergency spillway for the first time since the dam was built. The subsequent near- failure of the emergency spillway resulted in the emergency evacuation of 180,000 residents from downstream of the dam. According to DWR, about 12.8 inches (325 mm) of precipitation fell on the basin between February 6 and 10, 2017. This period saw the maximum daily volume of water stored in the reservoir since at least February 1985, the date of the oldest data available on the California Data Exchange Center (CDEC, see http://cdec.water.ca.gov/). Repairs to both spillways are estimated to cost in excess of $500 million USD [2].

Orographic effects on the Feather River also pose a modeling challenge. Most traditional hydrologic models use a lumped-calibrated approach, where a given set of parameters are applied to broad geographic areas and tuned based on streamflow observations at the outlet of a basin [31]. However, the deep and narrow canyon that the North Fork follows below Lake Almanor often captures and funnels incoming winter storms. As the storms rise and their moisture condenses, they drop large amounts of precipitation on the ridges above the canyon. As a result, measurement stations such as Bucks Lake (CDEC code BKL) and Four Trees (FOR) regularly compete for the wettest locations in California (again, see http://cdec.water.ca.gov/). The relatively coarse resolution of many models can complicate the identification of these important intra-basin patterns, especially with respect to orographic precipitation and flow.

2.3 Project Objectives

The stated goals (and steps) of the project are as follows:

1. Create an intelligent water-information system to optimize real-time knowledge of hydrology across the landscape.

2. Use this system to provide more-detailed water-basin storage information.
3. Leverage this advanced monitoring capability to improve current runoff predictions and forecasting on the North Fork of the Feather River.
4. Demonstrate the actual cost savings from using this decision-support chain for Feather River stakeholders, including utility companies and water agencies.
5. Ultimately, contribute to mitigate the effects of climate change on California hydropower generation.

The core component of the intelligent water-information system (objective 1) is represented by wireless sensor networks (WSNs), a new type of environmental sensing infrastructure [61]. By measuring weather, snow, and soil data at physiographically representative locations within 1 km^2 patches (0.386 mi^2), these networks can complement existing standard index stations like snow pillows, which are usually installed in flat, open sites [15]. As we detail in Section 3, wireless sensor networks are constituted by multiple measurement or sensing nodes, which communicate using a wireless network. Data are transmitted to a base station, which sends them in real time to a remote server, available for users like forecasters. Previous prototype applications on the American River and at Providence Creek in southern Sierra have already proven that such networks can reliably provide multi-year hydrologic data at various scales [62,74].

A specific challenge is to convert data measured from wireless sensor networks to more significant hydrologic scales, e.g., the entire North Fork of the Feather River (objective 2). This goal points to synergy between data collected on the ground and monitoring tools like remote sensing, which have high spatial but low temporal resolution [17]. The working hypothesis is that blending data from wireless sensor networks with, e.g., MODIS snow covered area products (https://nsidc.org/) or Lidar scans (https://aso.jpl.nasa.gov/) can enhance the value of both datasets and provide coherent pictures of snow patterns at unprecedented spatial and temporal scales. Because the necessary resolution of these decision-support tools should be relatively high (say, comparable to the extension of single wireless sensor networks) and because such products should be available in real time, an effective data system must be put in place to manage large amounts of data.

Next, this project aims to demonstrate that such advanced spatial information can effectively improve hydrologic predictions (objective 3). Current runoff forecasting tools in California mainly rely on statistical regressions between historical peak snowpack, precipitation, and streamflow [47]. These approaches lack the necessary physical base to cope with changing climatic conditions and/or extreme precipitation. Complex rainfall-runoff models are a promising tool, but often lack details about the spatial distribution of input variables as well as basin properties. Data could be assimilated with model outputs to lessen data and prediction uncertainty.

Objective 4 is the real testing ground for wireless sensor networks. From a hydrologic perspective, the amount of available data is usually considered a determinant driver of model performance. From an economic perspective,

however, collecting data represents an additional overhead. The value of data and of monitoring networks must be therefore justified in a cost-benefit framework. Ultimately, the project aims to quantify the return of investment of the intelligent water-information system. This step will assess the economic value of advanced hydrologic information and will evaluate the financial added-value of high-resolution data. The project will demonstrate if and to what extent detailed hydrologic information can offset the risks and associated costs of hydropower as an energy resource in California.

3: Methods and Key Findings

3.1 Real-Time Intelligent Water-Information System

3.1.1. Overview of Methods

The first step of the project has been the deployment of four wireless sensor networks over the North Fork of the Feather River (see objective 1 and Section 3.1.3 for a description of the WSNs). Our site selection process over the Feather River was driven by a desire to expand current monitoring capabilities on the North Fork, where most of the powerhouses are located, with particular focus on the under-monitored and largely undeveloped East Branch. Networks – from here also referred to as clusters or sites – were chosen to be co-located with existing snow pillows that measure snow water equivalent (SWE). These sites where chosen together with PG&E and DWR. Co-located SWE measurements enable better estimation of snow-water storage across the landscape as well as comparison between WSNs and traditional monitoring tools. Sites were also chosen to sample along a large elevation gradient, as hydrologic processes in mountainous regions are driven by factors that change with elevation. Finally, sites were selected to capture hydrologic variability induced from orographic effects, including the ridge between the North Fork and the East Branch of the Feather River (see Section 2.1.1).

Next, the measurement locations within each cluster were identified based on a combination of hydrologic and network considerations. The goal was to find 12 locations (based on budgetary considerations) within the 1 km^2 deployment area (0.386 mi^2) that capture the variability of factors known to affect snow cover: slope, aspect, vegetation, and elevation. This was done by a machine-learning program developed in our laboratory [44]. One measurement station per site was installed at the location of the snow pillow to enable direct comparisons between our measurements of snow depth and pillow SWE (henceforth, this node is referred to as the pillow node). At the same location, a shielded rain gauge is available.

Section 3.1.2 describes the characteristics of each cluster in more detail. Section 3.1.3 describes the hardware used by wireless sensor networks to measure and transmit data in real time. Examples of hydrologic data measured during water year 2017 are provided and compared to standard hydrologic data at co-located snow pillows in Section 3.1.4. We comment on the key findings and implications from a forecasting perspective in Section 3.1.5 Details about the software used to

manage the measurement nodes and transmit data in real time can be found in [36][1].

3.1.2 Deployments

The chosen measurement sites are Bucks Lake (BKL, latitude 39.85N, longitude 121.242W, elevation 5750 ft /1750 m), Grizzly Ridge (GRZ, latitude 39.917N, longitude 120.645W, elevation 6900 ft / 2100 m), Kettle Rock (KTL, latitude 40.14N, longitude 120.715W, elevation 7300 ft / 2220 m), and Humbug (HMB, latitude 40.115N, longitude 121.368W, elevation 6500 ft / 1980 m). The Bucks Lake, Grizzly Ridge, and Kettle Rock clusters were installed during the summer of 2016. The Humbug cluster was installed during the summer of 2017. This report includes results based on data from BKL, GRZ, and KTL.

Tables 1 through 4 summarize the topographic features of the sensor station locations in each deployment. The number in the "Sensor Station" column refers to the locations shown in Figure 4. "Slope" indicates the slope of the ground at the sensor station location. "Aspect" indicates the orientation of the slope relative to North. "Vegetation" indicates the percentage of vegetation at the sensor station location, which was estimated basing on the National Land Cover Database (NLCD) canopy dataset (https://www.mrlc.gov/). The original 30 m cell size of the NLCD dataset was downscaled to 10 m using bilinear interpolation for the scope of this work. Figure 4 shows a bird's eye view of the deployments.

3.1.3 Measurement System

Four different types of hardware are used in these deployments:

- Sensor stations (Figure 3a) are installed at physiographically representative locations within each network clusters and measure snow and meteorological variables, which are transmitted to the base station.
- If the sensor station is too far away from the base station for direct communication, repeater nodes (Figure 3b) are installed to serve as data relays.
- The base station (Figure 3c) serves as a collection point for all the data gathered by the sensor stations and forwards these data to the server over a cellular Internet link.
- The server receives, stores, and displays the data (not shown).

Each type of hardware is detailed below. Circled numbers (e.g. ①) refer to annotations in Figure 3.

[1]This section includes excerpts from the following paper: http://www.mdpi.com/1424-8220/17/11/2583

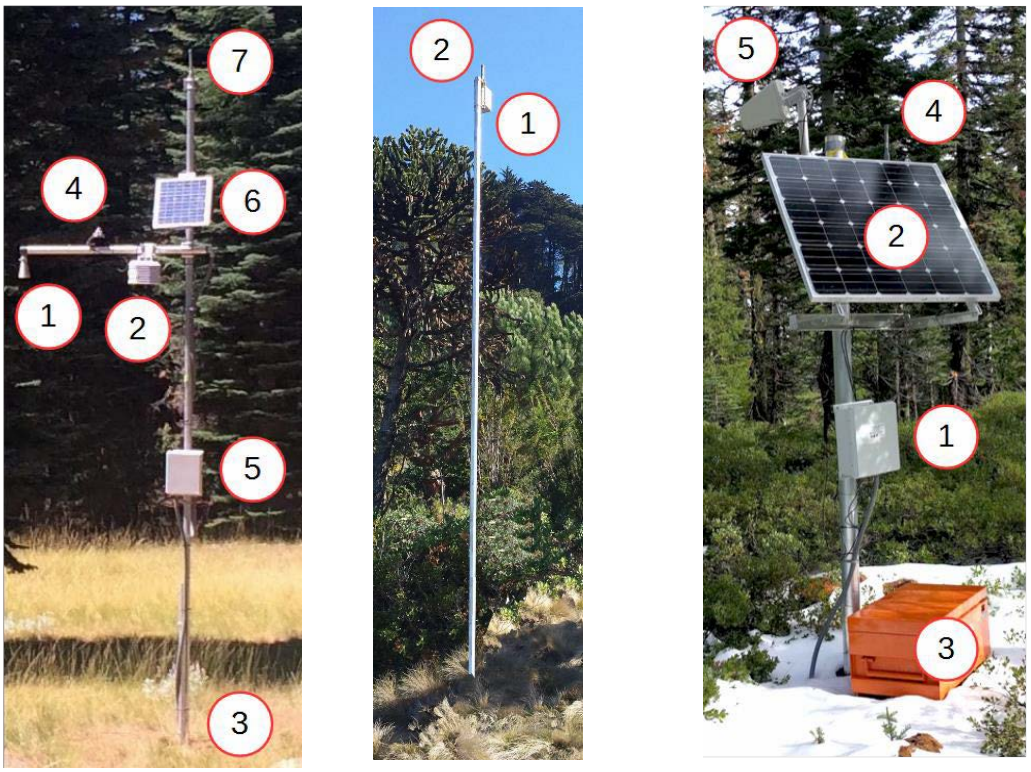

(a) *(b)* *(c)*

Figure 3: The hardware used. Circled numbers refer to specific modules of the system in Section 3.1.3. (a) Sensor station; (b) Repeater node; and (c) Base station.

Sensor Station: A sensor station (Figure 3a) consists of an aluminum pole with sensors attached and a mote to control the sensors, make local calculations, and communicate the sensor measurements to the base station. Up to four types of sensors are mounted onto the pole:

- An MB7363 MaxBotix ultrasonic range-finder (①) is mounted on the tip of the cross arm, oriented downwards. It measures the distance to ground or snow by measuring the round-trip time of an ultrasonic pulse. It has a resolution of 1 mm (0.04 inches), an accuracy of 1%, and a range of 50 cm to 10 m (1.64 to 33 ft). Like all ultrasonic devices, it is less accurate while it is snowing.
- Temperature and relative humidity are measured by a Sensirion SHT25 sensor ②. It is enclosed in a radiation shield and mounted about halfway across the cross arm.
- Decagon GS3 soil moisture sensor ③ which measures soil dielectric constant, electric conductivity and temperature. Soil moisture is more accurately estimated via a calibration relation (see http://manuals.decagon.com/Manuals/13822_GS3_Web.pdf). Results reported have not been locally calibrated. Two such sensors are installed per

sensor station, at depths of 25 cm and 50 cm into the ground (0.82 and 1.64 ft, respectively).

- One Hukseflux LP02 pyranometer solar radiation sensor ④ is installed per WSN in an open area. Unshaded solar radiation tends to be uniform across a 1–2 km^2 area (0.38 – 0.77 mi^2).

These sensors are connected through wires to a managing NeoMote by Metronome Systems (http://www.metronomesystems.com/), a multi-purpose, ultra-low mote housed in ⑤. An omnidirectional antenna is mounted on the top of the pole (⑦) to allow the wireless module to communicate with other components of the network. The sensor nodes are powered by a twelve-pack lithium ion battery and a solar panel (⑥).

Repeater Node: The role of the repeater node (Figure 3b) is to provide connectivity between the sensor stations and the base station and maintain redundancy in the mesh network. It is more simple than a sensor station, as it only contains a waterproof fiberglass enclosure (①) with a Metronome Systems Wireless Sensing Relay Board. An antenna is mounted on the top of the box (②).

Base Station: The base station (Figure 3c) serves four roles: (i) control and maintain the network, (ii) collect the sensor measurements from the sensor stations via radio antenna (④), (iii) locally store the data, and (iv) transmit the data to the server on the Internet through a cellular connection (⑤). Electronics are housed in ①, while power comes from the solar panel (②) and batteries housed in ③.

Within each target site, the base station was placed in an area of high cellular connectivity and as close as possible to the center of the field site. This placement minimizes the number of connections to the farthest nodes in the final mesh network, reducing power consumption and increasing reliability. Given multiple potential sensor station locations, we preferred locations that are close to the base station to limit the number of repeaters.

Server: The server serves three roles: (i) receive the data sent by the base stations of multiple deployments; (ii) store the data in a database; and (iii) offer a web interface to navigate and download the data.

Table 1: Sensor station features: Bucks Lake

Sensor Station	Elevation, ft (m)	Slope, °	Aspect, °	Vegetation, %
0	5748 (1752)	5	238	70
1	5705 (1739)	13	272	60
2 (pillow)	5803 (1769)	0	158	50
3	5626 (1715)	15	277	70
4	5800 (1768)	2	109	70
5	5754 (1754)	10	319	60
6	5583 (1702)	17	222	80
7	5810 (1771)	2	133	70
8	5751 (1753)	4	90	20
9	5695 (1736)	8	324	40
10	5577 (1700)	14	339	80
11	5721 (1744)	4	54	70

Table 2: Sensor station features: Grizzly Ridge

Sensor Station	Elevation, ft (m)	Slope, °	Aspect, °	Vegetation, %
1 (pillow)	6833 (2083)	5	15	10
2	6768 (2063)	11	54	70
3	6893 (2101)	5	102	50
4	6551 (1997)	15	58	60
5	6883 (2098)	18	348	70
6	6919 (2109)	10	328	50
7	6807 (2075)	6	109	40
8	6827 (2081)	3	73	20
9	6624 (2019)	11	48	50
10	6938 (2115)	7	324	50
11	6610 (2015)	12	59	40
12	6791 (2070)	16	39	70

Table 3: Sensor station features: Kettle Rock

Sensor Station	Elevation, ft (m)	Slope, °	Aspect, °	Vegetation, %
1	7309 (2228)	18	196	40
2	7345 (2239)	8	231	40
3	7467 (2276)	12	153	40
4	7122 (2171)	15	180	90
5	7211 (2198)	14	54	30
6	7106 (2166)	14	154	60
7 (pillow)	7250 (2210)	8	179	0
8	7329 (2234)	15	99	0
9	7273 (2217)	11	213	50
10	7076 (2157)	9	156	60
11	6991 (2131)	15	180	60
12	7329 (2234)	12	14	30

Table 4: Sensor station features: Humbug

Sensor Station	Elevation, ft (m)	Slope, °	Aspect, °	Vegetation, %
0	6666 (2032)	2	37	70
1	6509 (1984)	11	39	70
2 (pillow)	6551 (1997)	5	151	10
3	6538 (1993)	1	63	60
4	6548 (1996)	3	169	40
5	6538 (1993)	2	37	70
6	6578 (2005)	6	168	60
7	6519 (1987)	2	167	60
8	6653 (2028)	6	16	60
9	6637 (2023)	11	174	70
10	6597 (2011)	9	17	60
11	6663 (2031)	4	165	70

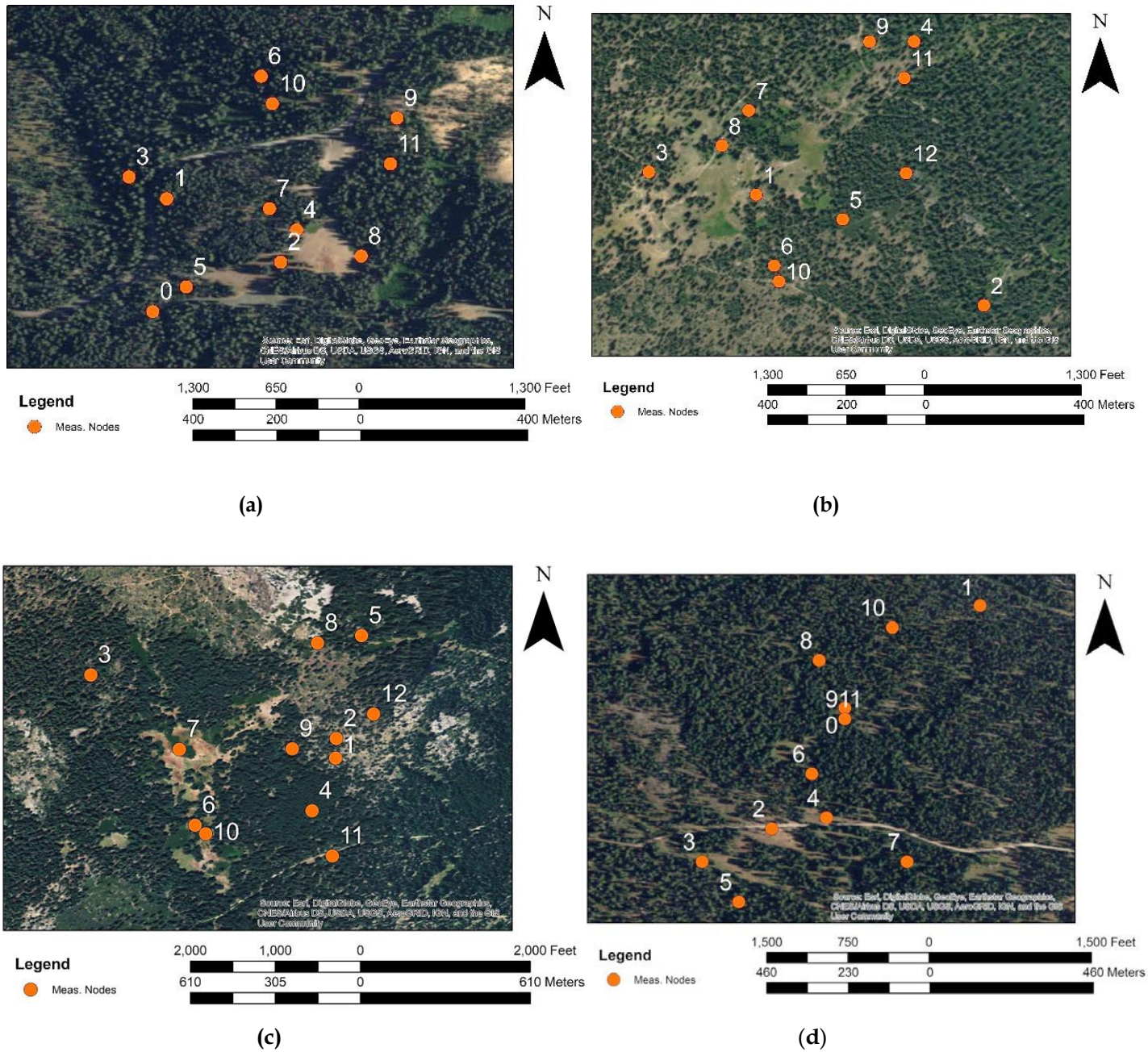

Figure 4: Maps of the deployments: (a) Bucks Lake; (b) Grizzly Ridge; (c) Kettle Rock; and (d) Humbug

3.1.4 Examples of Hydrologic Data

Figure 5 shows an example of mid-winter sensor data from Grizzly Ridge beginning 15 January 2017 and ending 1 March 2017. Figure 6 shows a second example from the same site spanning from 1 May 2017 to 15 June 2017 (snow melt season). These two timeframes are used to exemplify the entire range of hydrologic fluxes and states that were monitored during the 2017 water year using wireless sensor networks. Data are freely available at the following link: http://frho.us/.

Accumulation Period: The 2016/2017 snow season at Grizzly Ridge started in mid-November. Only a shallow snowpack persisted until 1 January (around 30 cm, data not shown). As mentioned, Northern California received exceptional snowfall in January and February [69, 70]. Due to complex topographic transitions between rainfall and snowfall, some of these precipitation events exhibited both an increase in snow depth and massive snow melt. An example of this effect is the rain-on-snow event between 6 and 10 February (see Section 2.2).

Figure 5 focuses on three of these large precipitation events. All nodes at the site show increasing snow depth (Figure 5a), saturated air (Figure 5c), and decreased solar radiation (Figure 5d) during the events. Readings are similar because precipitation occurs over a much larger area than the area covered by the nodes. Based on measurements of snow depth and air temperature at nodes, these events can be classified as either snowfall (18 January 2017 to 22 January 2017 and 19 February 2017 to 20 February 2017) or mixed rain and snow (3 February 2017 to 9 February 2017). Blending sensor information and co-located rain gauge data obtained from CDEC shows occurrences of rainfall after 8 February 2017, when snow depth at nodes started to decrease but the rain gauge recorded an increase. These three precipitation events were separated either by periods of possible snow melt (30 January 2017 to 31 January 2017, indicated by decreasing snow depth and temperatures above 32 °F, or 0 °C) or settling (25 January 2017 to 28 January 2017, indicated by decreasing snow depth and temperatures below 32 °F, or 0 °C). Snow melt and settling have different implications for runoff forecasting in snow-dominated regions.

Simultaneous soil moisture data (Figure 5e–f) show no significant infiltration during the two snowfall events but marked variability of soil moisture between nodes during the February rain-on-snow event. These changes in soil moisture may be related to differences in moisture conditions across nodes and in precipitation phase (rain vs snow) at local scale. While nodes recorded stable winter soil temperature at seasonal scale (between +34 and 37.5 °F, or +1 and +3 °C), some of them showed either decreasing or increasing soil temperature from 7 February 2017 to 10 February 2017, which could be related to local-scale energy processes during rain-on-snow events like snowpack phase change, soil thawing, or rainfall temperature.

Snow Melt Period: The 2017 snow melt season in Grizzly Ridge started in March. Depending on the location, canopy coverage, and peak snow depth of nodes, the end-of-season date ranged between 13 May 2017 (Node 9) and 6 June 2017 (Node 4). Figure 6 focuses on this key period of the water year when snowmelt runoff represents an important input to the surface and sub-surface hydrologic systems of Californian Alpine watersheds.

All nodes showed a constantly decreasing snow depth during the period considered (Figure 6a). This decrease is consistent with simultaneous daily cycles in solar radiation (Figure

6d), relative humidity (Figure 6c), and temperature (Figure 6b), which are all proxies of stable atmospheric conditions and absence of precipitation (confirmed by the co-located rain gauge). The only period of constant snow depth was recorded between 14 May 2017 and 17 May 2017 and was marked by simultaneous below-freezing air temperature, saturated air, and decreased solar radiation. While these conditions might be indicative of precipitation, a cross-check with snow depth readings (which were constant) and co-located soil moisture readings (which were decreasing at most nodes) can exclude significant precipitation events during this time in agreement with the co-located rain gauge.

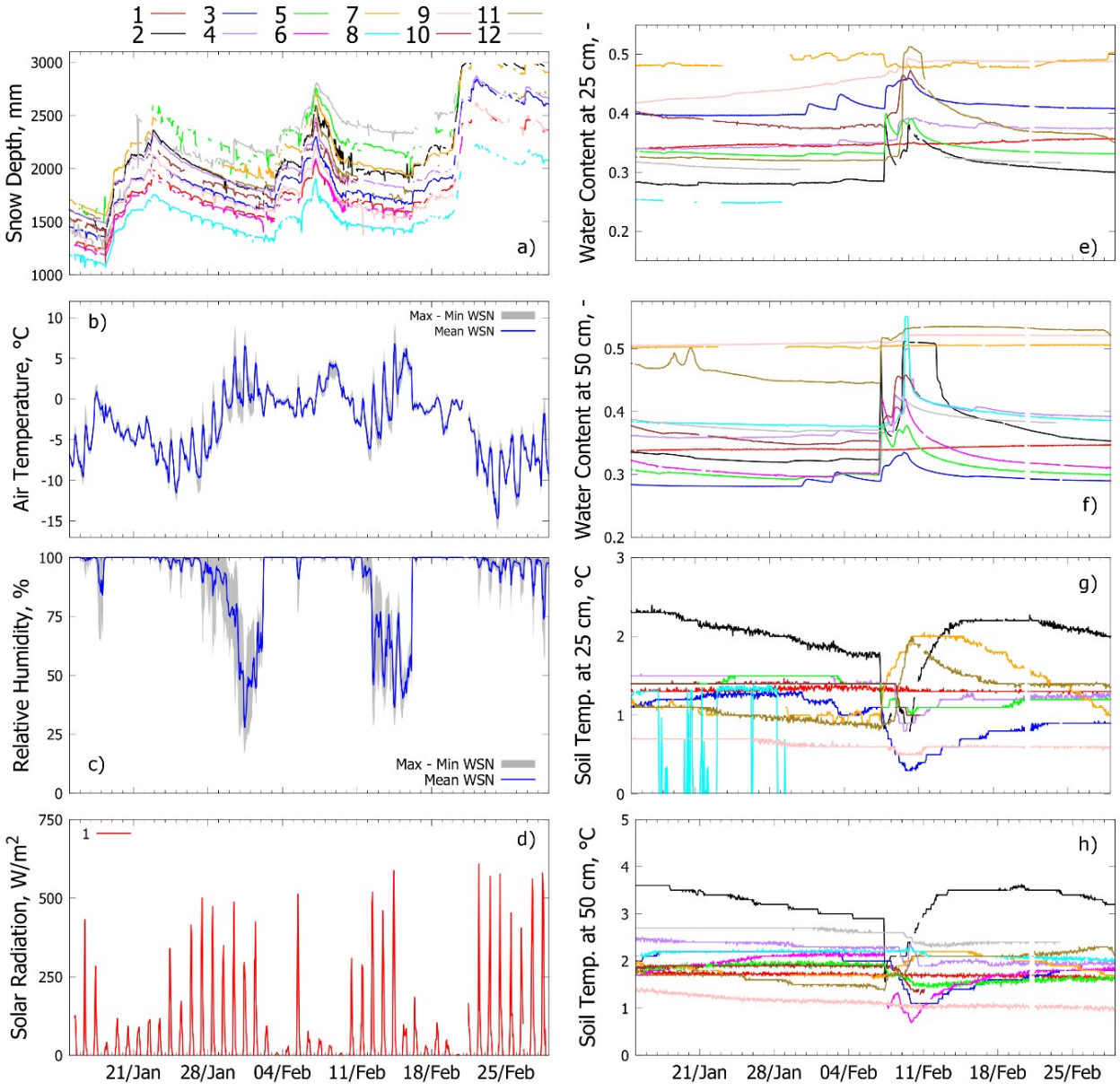

Figure 5: Examples of mid-winter raw sensor data from Grizzly Ridge (15 January 2017 to 1 March 2017). Line colors for panels (e–h) are the same as panel (a). Because measurements of air temperature and relative humidity show relatively small variability within nodes, panels (b, c) only report maximum-minimum range and mean. Solar radiation is only measured at node 1

(pillow) and shown in (d). Soil water content in in volumetric fraction. Ranges in customary units are as follows: panel (a) 3.29 to 9.84 ft (1000 to 3000 mm); panel (b) 5 to 50 °F (-15 to 10 °C); panel (g) 32 to 37.4 °F (0 to 3 °C); panel (h) 32 to 41 °F (0 to 5°C)

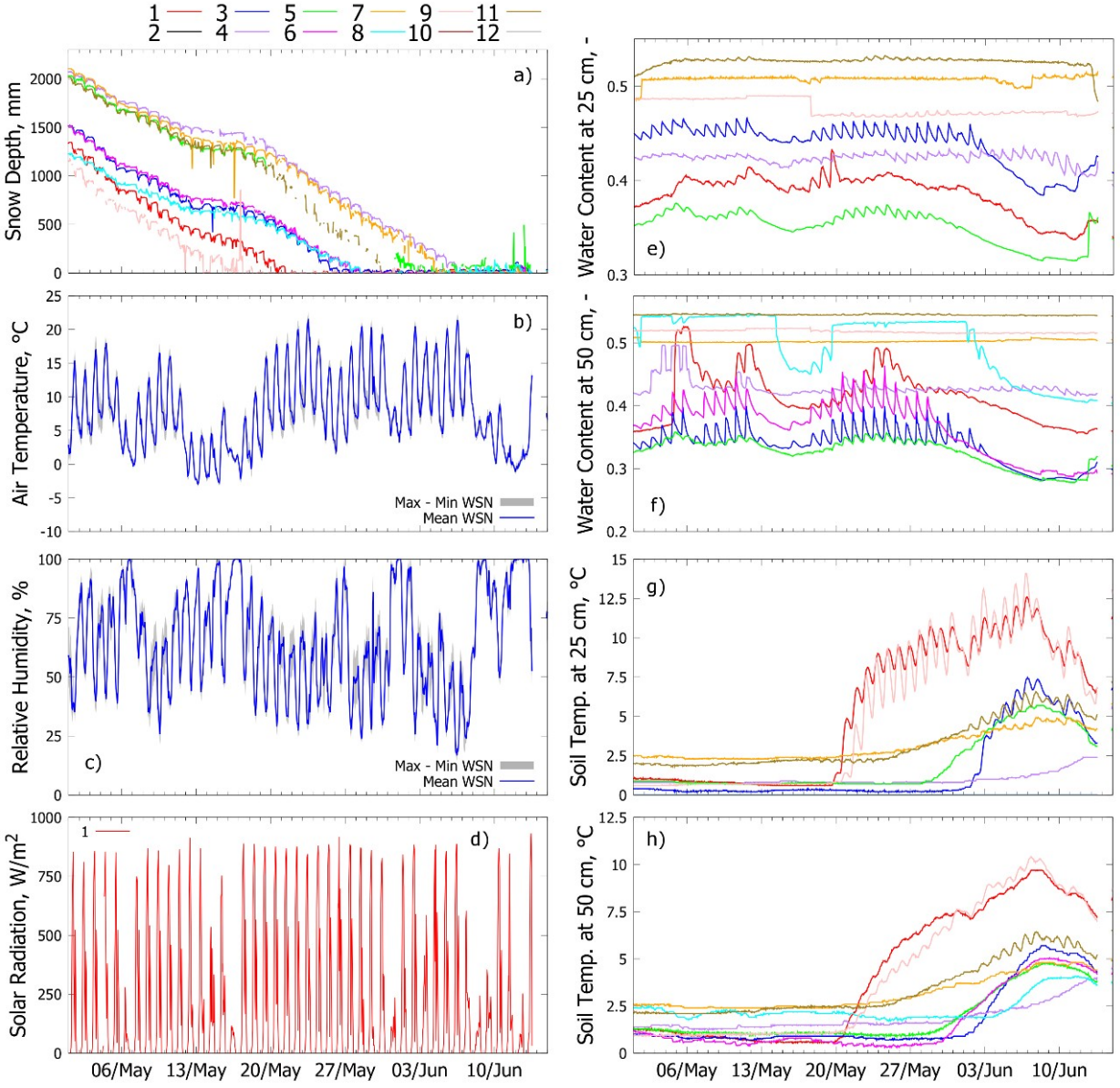

Figure 6: Examples of spring raw sensor data from Grizzly Ridge (1 May 2017 to 15 June 2017). Line colors for panels (e–h) are the same as panel (a). Because measurements of air temperature and relative humidity show relatively small variability within nodes, panels (b,c) only report maximum-minimum range and mean. Solar radiation is only measured at node 1 (pillow) and shown in (d). Soil water content in in volumetric fraction. Soil water content and temperature sensors at 25 cm depth (0.82 ft) malfunctioned at both nodes 6 and 8 during the reported periods. These data are therefore missing in panels (e) to (h). Ranges in customary units are as follows: panel (a) 0 to 6.65 ft (0 to 2000 mm); panel (b) 14 to 77 °F (- 10 to 25 °C); panel (g) 32 to 59 °F (0 to 15 °C); panel (h) 32 to 60 °F (0 to 12.5 °C)

The end-of-season date was marked by diurnal soil temperature cycles that were not observed during periods of snow on the ground (Figure 6g–h, [35]). Soil moisture showed clear differences in daily temporal patterns between nodes (Figure 6e–f); while some nodes show recharge-discharge dynamics due to snow melt infiltration into the ground, others show constant saturation, which may have impeded infiltration and caused surface runoff. After snow disappeared, soil moisture decreased at most nodes due to the absence of inputs from the ground surface and concurrent evapotranspiration.

Comparison with Snow Courses: Figure 7 compares the range of variability of snow depth measurements with data taken by manual monthly snow courses at the same locations (no snow courses are done at the Bucks Lake site). Snow courses are performed by manually measuring snow depth along transects and averaging measurements to provide a representative value for the site. Maximum, average, and minimum daily snow depth across all nodes at each network were calculated when eight or more different node values are available. For the purposes of comparison, we selected the depth recorded by the sensor node placed at the snow pillow.

The data show similar patterns: accumulation occurs from December to February, peak accumulation in March, and snow melt from April to May. Snow courses, however, tend to overestimate the mean site snow depth and may even exceed the maximum measurement from sensor nodes. Due to their coarse temporal resolution, snow courses do not provide important hydrologic statistics such as date of peak snow or snow melt-out date. The WSN data reveal that spatial variability increases over time in response to differing solar radiation inputs across the nodes. This solar radiation variability is due to different vegetation coverages and slope aspects (i.e., the slopes face different directions). This considerable variation cannot be captured by a single index station. Maximum differences in snow depth are on the order of 5 to 6.5 ft (1.5 to 2 m), resulting in significantly different end-of-season dates from node to node. Snow melt is the primary driver of streamflow during the ablation period, and this timing difference may significantly impact runoff forecasting.

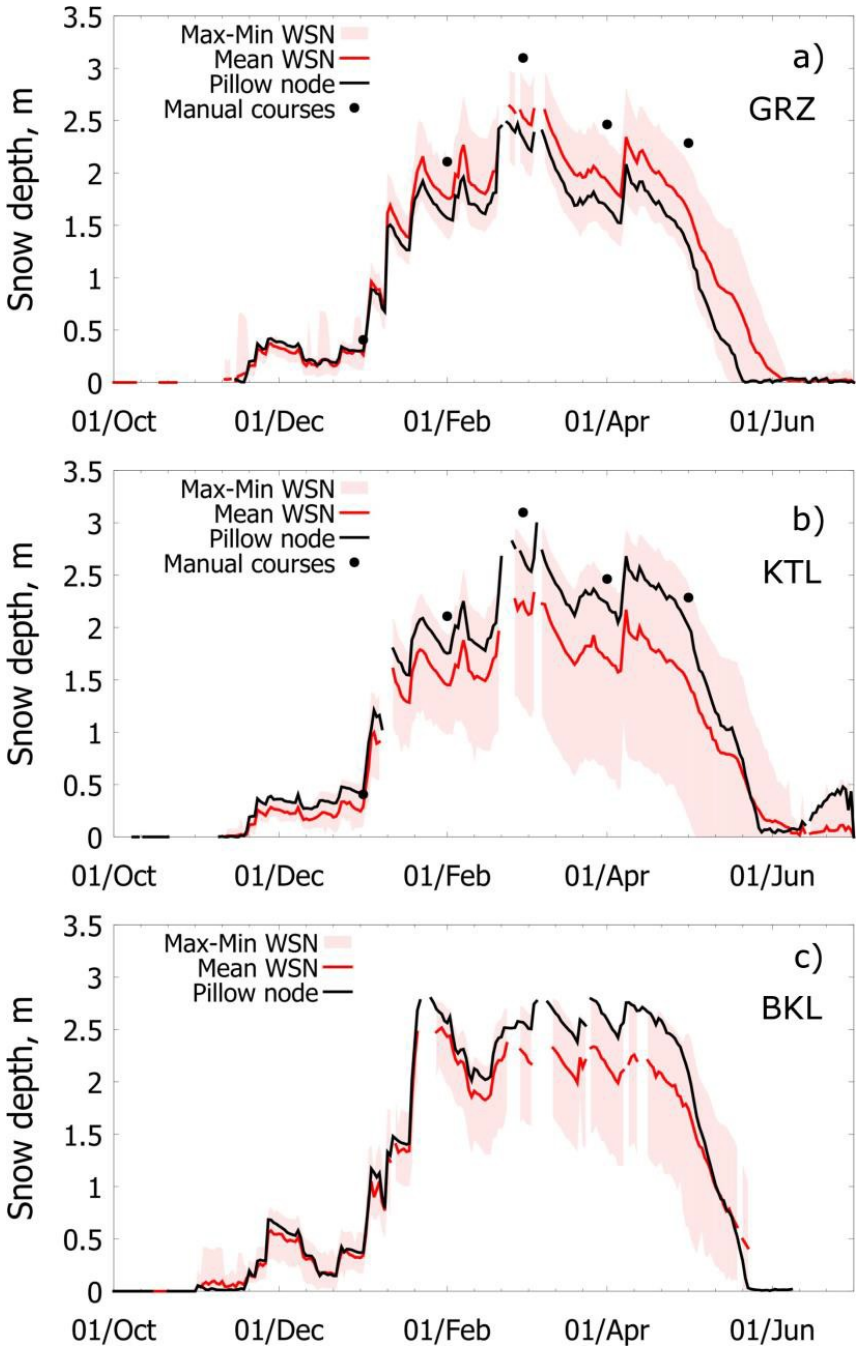

Figure 7: Comparison between snow depth measurements from wireless sensor networks (red and black) and manual measurements taken by monthly snow courses (dotted black) at the same locations (water year 2017): Grizzly Ridge (a), Kettle Rock (b) and Bucks Lake (c) 1, 2, and 3 m correspond to 3.28, 6.56, and 11.5 ft, respectively.

3.1.5 Forecasting Value

These results show that wireless sensor networks provide several important advantages when compared with traditional index stations. First, traditional index stations show a significant bias in terms of both peak accumulation and snow melt rate. Standard instrumentation, especially snow pillows, are typically located in areas that are flat and free of vegetation, making them less representative of snow distribution in mountain regions like the Sierra Nevada, which is largely covered by forests and characterized by complex topography [62]. As a result, snow pillows can track the mean timing of melt but fail to capture snow-melt or accumulation variability. Due to their large size and their impervious surface, snow pillows also prevent infiltration into the ground from the snow they are measuring and insulate snow from thermal exchanges with soil. This disconnection affects data such as end-of-season date and snow-melt rate. The end-of-season date is an important metric for hydropower and water supply forecasters, as it signals a shift from snow melt- dominated runoff towards other processes like groundwater discharge and evapotranspiration.

Blending data from wireless sensor networks and co-located, standard instrumentation also allows us to detect precipitation timing and phase, which can be critical in determining subsequent streamflow peaks. This feature can compensate for some well-known problems with traditional sensors. For example, rain gauges provide information on precipitation amount, but not phase. They are also prone to underestimating precipitation during intense snowfall/rainfall events due to wind effects and plugging. Another example is infiltration; most existing networks do not routinely measure soil moisture, whereas these systems do. Since overland flow is a much faster process of streamflow generation than infiltration, soil moisture information can support short-term runoff forecasting at downstream reservoirs and powerhouses.

Finally, results show that vegetation has a significant impact on snow depth changes, creating heterogeneity even across small spatial scales. The variety of data collection sites in this project allow data collected under specific features to be generalized to ungauged areas with similar conditions. Due to the complex interaction between snow melt and topography in mountain watersheds, data collected by traditional instruments are nearly impossible to distribute.

3.2 Hydrologic Data Information System

3.2.1 Overview of Methods

The second project objective focuses on developing the ability to combine WSN data (Section 3.1.4) with remote sensing, machine learning, and data integration techniques to expand the information from point measurements and create spatial maps of conditions during the winter (see Section 3.2.2). Because sensor node locations were picked to be representative of a range of environmental conditions, we can extrapolate data beyond the locations of the nodes or even the clusters themselves. Of particular interest is a map of snow water equivalent across the landscape on any given day. In Section 3.2.3, we also describe efforts to make the data available to the public, Feather River stakeholders, and other researchers to maximize the potential benefits of the project.

3.2.2 Blending Ground-based and Remote-sensing Data: Snow Maps

In the Feather River basin, we identify ten stations (CDEC codes BKL, KTL, GRZ, FOR, HMB, LLP, PLP, GOL, RTL, and HRK) providing hourly SWE and other hydrologic

measurements, including temperature, humidity, or precipitation. NASA's MODIS and LANDSAT missions provide us spatial information of snow cover, but not its water equivalent. Figure 8 shows the locations of SWE stations and of WSNs, overlaid on a historical SWE map for context [20, 37].

Estimating SWE distribution across the basin given these sparse observations is not a trivial task. However, although SWE has high spatial variability, its spatial patterns are somewhat preserved year-to-year [63]. We discuss two methods for potentially real-time estimation of SWE across the Feather River Basin. The first approach leverages the similarity in snow pattern between different years. It consists of two operational steps that need to be executed daily. It also requires a historical SWE product [20, 37], real-time SWE observations (like CDEC and WSNs), and, optionally, remotely-sensed fractional snow cover (MODIS) [85].

First, a prior estimate of the SWE map is computed using a nearest neighbor (NN) approach with historical maps [20, 37]. In other words, we find the historical SWE map that provides the most similar SWE distribution to that measured at the sensor locations. This step constitutes the background SWE map or prior estimate. Observations are also collected from CDEC (http://cdec.water.ca.gov/) and the WSNs.

Second, an Ensemble Optimal Interpolation (EnOI) scheme [14] is used to distribute the residuals across the region between the observed locations and the prior estimate. Observations for this step include real-time SWE stations aggregated to daily averages (including WSN nodes, where SWE is estimated by calculating daily density at the pillow node and then assuming daily density to be the same for all nodes at the same site). This method depends on the choice of background error statistics and is designed for statistical systems. Correlations between SWE at different locations are indirectly estimated from the static historical data ensemble used, which includes maps from 2010 to 2016. The ensemble is reduced to 100 images using eigenvalue decomposition to reduce simulation time and storage requirements. Taken together, these steps are referred to as the NN-EnOI scheme. The grid size is 100 x 100 m (328 x 328 ft).

As an example, Figure 9 shows the estimated SWE map for April 1, 2017, the canonical date in snow hydrology for peak SWE accumulation (http://cdec.water.ca.gov/). Figure 10 also shows the reconstructed MODIS fractional snow cover map for the same day. These maps will be made available on the FRHO website at http://frho.us/.

To evaluate the performance of this method, we performed a leave-one-out cross validation: we sequentially excluded data from the snow pillows at HMB, RTL, PLP, KTL, GRZ, and BKL from the algorithm and ran the simulations. In KTL, GRZ, and BKL we also removed data from all WSN nodes, even though this step significantly reduced the amount of available data for reconstruction. Data from each of these sites can then be used as separate evaluation datasets. Figures 11 and 12 show SWE reconstructions compared to the observed data at two of these locations, HMB and RTL. Appendix B includes results in PLP, KTL, GRZ, and BKL (Figures B-1 to B-4).

Root mean square errors (RMSE) for HMB, RTL, and PLP (where data from WSN were used in reconstruction, a more realistic scenario for future operational procedure) are 3.41 inches, 2.33 inches, and 11.62 inches, respectively (86.8 mm, 59.1 mm, and 295.1 mm). Peak SWE at each of these sites was approximately 51 inches, 31 inches, and 75 inches (1300 mm, 800 mm, and 1900 mm), meaning that RSME is about 6.7% of peak SWE for HMB, 7.3% for RTL, and about 15.5% for PLP. Importantly, the NN-EnOI method shows

promise for representing both the snow accumulation and ablation seasons; traditionally, the ablation season has been harder to capture due to multiple factors affecting snow melt rate. This phenomenon is reflected in the wide variation in melt-out date identified at WSN sites (see Section 3.1.4 and Figure 7). RMSEs of less than 10% of peak SWE are promising, with results at PLP only being slightly less accurate. Results at WSN locations (Fig. B-2 to B-4) confirm these conclusions and show robustness to a significantly smaller amount of data. Future steps, which are briefly described below, will aim to introduce further blending techniques to improve these results.

This second method, now under development, consists of assimilating NN-EnOI maps and ground-based standard hydrologic data with PRMS, the hydrologic model currently in use by PG&E and DWR on the Feather River (see Section 3.3). Model–data assimilation will allow us to combine the physical realism of ground-based data, the improved spatial reconstruction of snow distribution from NN-EnOI maps and from satellites, and a robust mass–energy conservation scheme of a dynamic model. The method we are currently developing relies on an ensemble Kalman filter (EnKF) to update model predictions at various scales with real-time data of SWE, snow depth, fractional snow cover from MODIS, and streamflow [84]. By leveraging *a priori* uncertainty information for both data and model outputs, EnKF will combine data and model simulations (potentially in real time) and quantify the uncertainty associated with the target output (such as streamflow). The main challenge we are currently addressing is how to correctly quantify uncertainty in input data and process-model outputs.

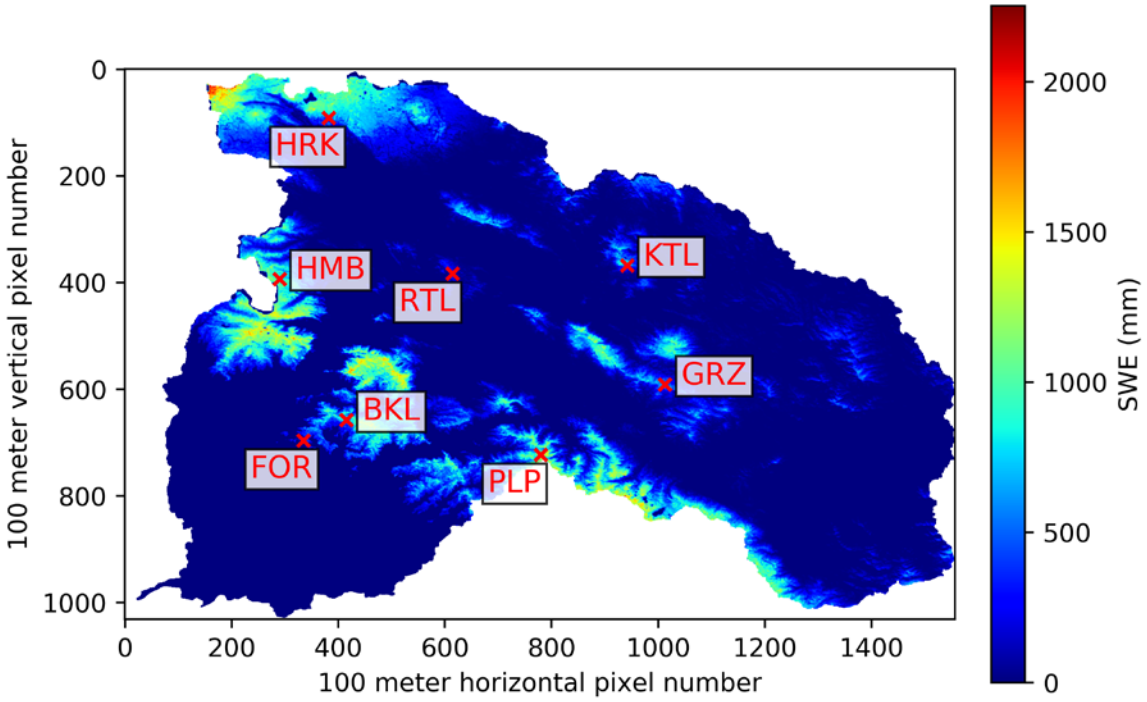

Figure 8: Locations of SWE stations and WSNs, overlaid on a historical SWE map for context (April 1st, 2016).

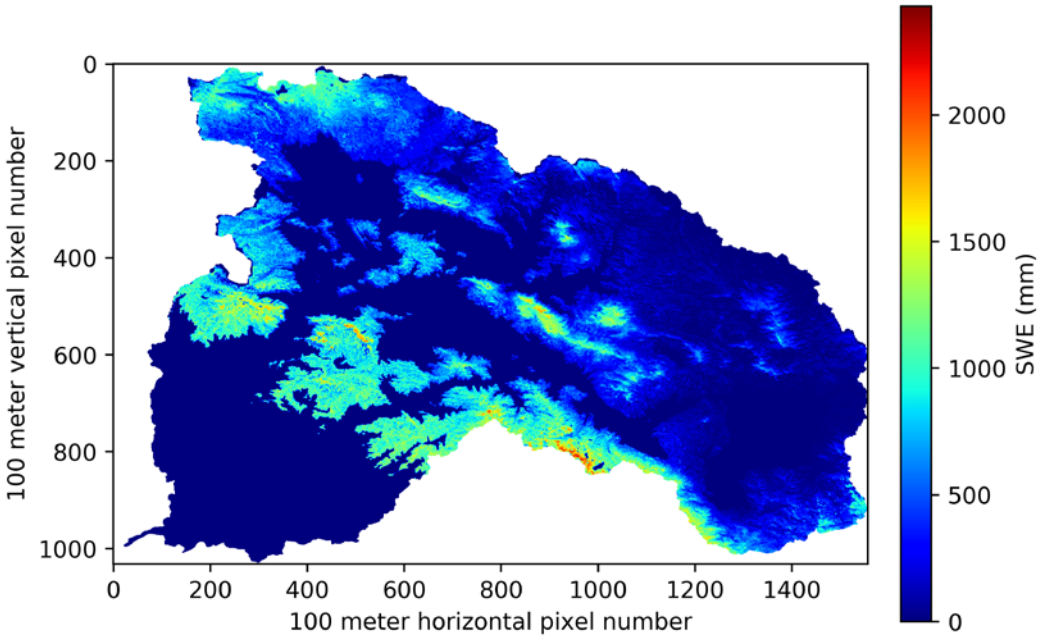

Figure 9: NN-EnOI estimation of SWE over the Feather River for April 1, 2017 (NN-EnOI stands for Nearest Neighbor - Ensemble Optimal Interpolation scheme). The color bar indicates SWE in millimeters. 1000 and 2000 mm correspond to 39 and 78 inches, respectively. Both the horizontal and vertical axes have units of 100 m (328 ft).

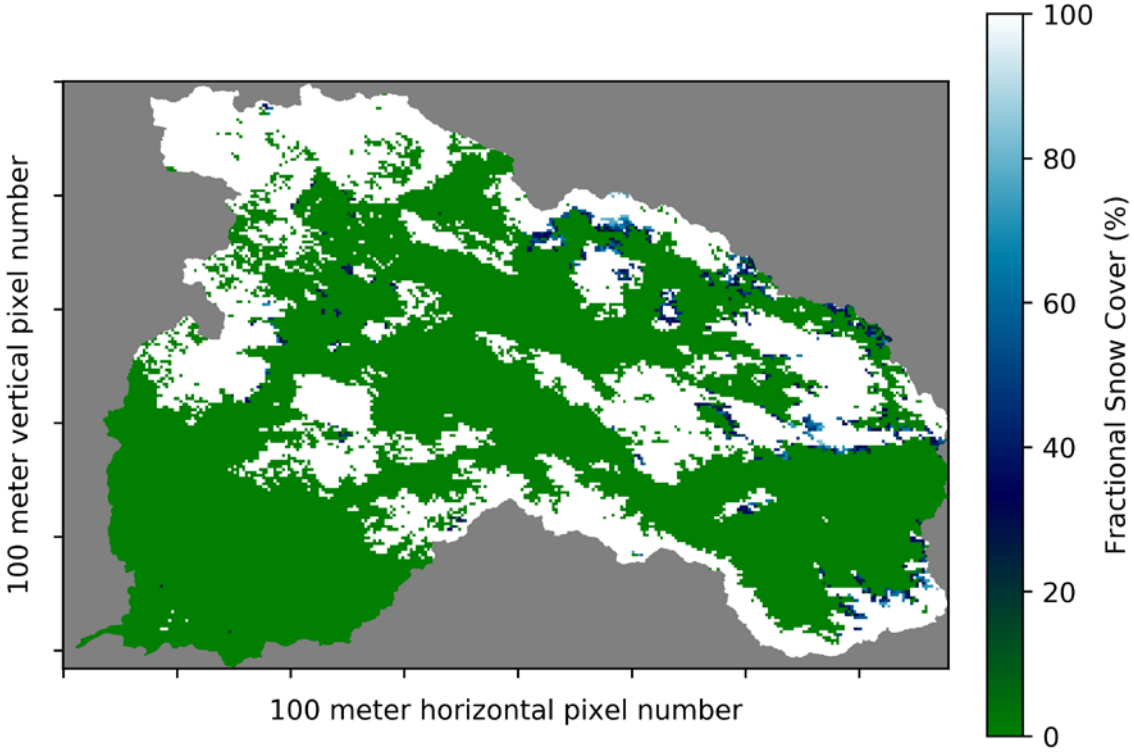

Figure 10: MODIS reconstructed fractional snow cover map for April 1, 2017. The color bar indicates fractional snow cover in percentage. Both the horizontal and vertical axes have units of 100 m (328 ft).

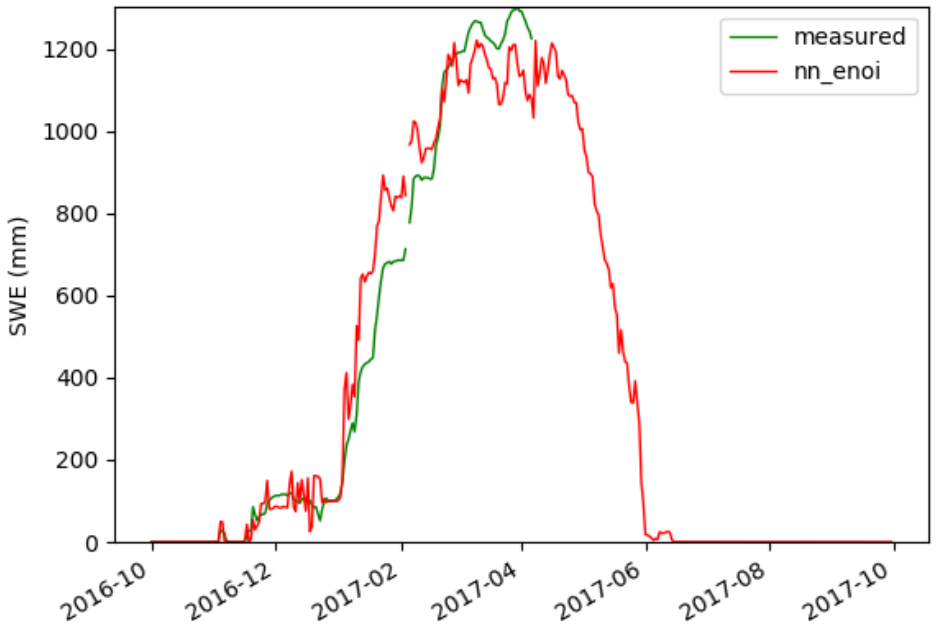

Figure 11: Humbug (HMB) snow pillow readings compared with NN-EnOI simulation (NN-EnOI stands for Nearest Neighbor - Ensemble Optimal Interpolation scheme). 500 and 1000 mm correspond to 19.7 and 39.37 inches, respectively.

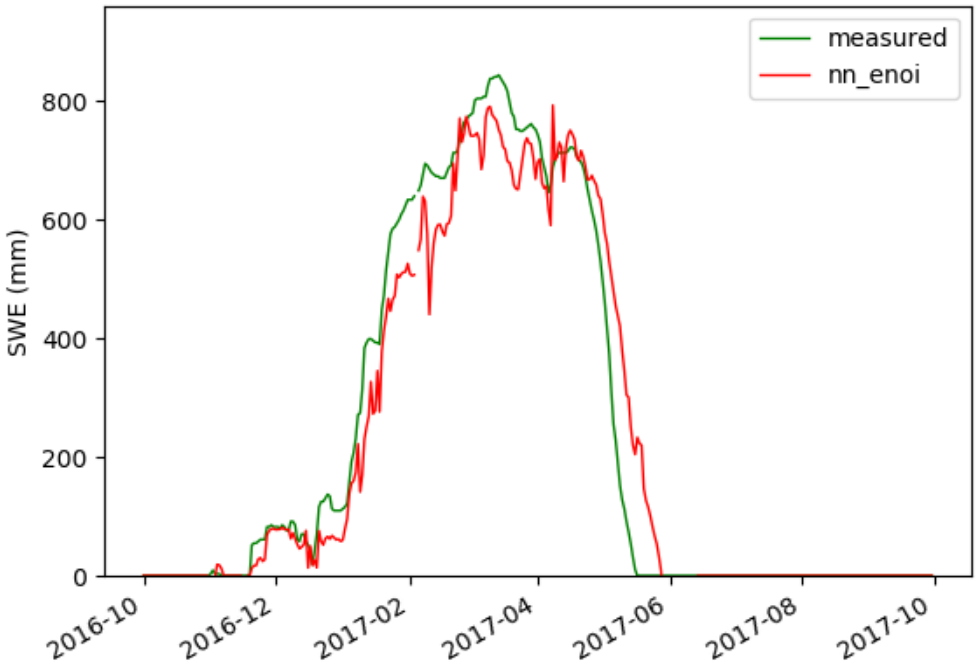

Figure 12: Rattlesnake (RTL) snow pillow readings compared with NN-EnOI simulation (NN-EnOI stands for Nearest Neighbor - Ensemble Optimal Interpolation scheme). 400 and 800 mm correspond to 15.74 and 31.49 inches, respectively.

3.2.3 Website

The Feather River Hydrologic Observatory website (http://frho.us/) provides a general overview of the project and includes access to real-time data. Of particular interest is the data section, which is further divided by the three sensor cluster locations. A fourth section will be added in the future for the site at Humbug, installed in the summer of 2017. Each section features an interactive Google map with sensor node and CDEC snow pillow coordinates. A select number of sensor nodes are also available to view on Google street view. Each section displays separate interactive graphs that incorporate real-time data from the sensor nodes with the following measurements: snow depth, relative humidity, soil temperature, and soil moisture. Graphs of CDEC data corresponding to the sensor cluster will also be included as a comparison to the sensor node data. The following measurements are available from CDEC at the daily and hourly timesteps: snow water equivalent and precipitation. The graphs are designed for ease of readability and to be easily understood by the public. Raw, unprocessed data may be downloaded by visitors to the site under the same data policy of the Critical Zone Observatories (http://criticalzone.org/national/data/czo-data-policies/).

3.2.4 Forecasting Value

The ability to generate real-time point measurements as well as SWE maps has the potential to vastly improve hydrologic modeling reliability. The first and most direct way this occurs is through more accurate data inputs to hydrologic models. Though such models can usually be run with only daily minimum and maximum temperature and daily precipitation, most of them are formulated in a modular framework, meaning additional data may be leveraged if it is available. The WSNs open the possibility of using these modules, which would mean the model relies on direct measurement rather than simplified calculations for these internal states. Use of such modules may also simplify the challenge of calibrating the model by reducing the overall number of parameters.

In addition to direct inputs, we are interested in using the blended SWE maps to make runtime changes to internal model variables. This process, known as data assimilation, will involve using the SWE maps to update model projections.

3.3 Hydrologic Modeling Improvements

3.3.1 Overview of Methods

The new real-time weather and snow data developed in Sections 3.1 and 3.2 are geared towards the improvement of water-related decision-support systems and towards overcoming limitations of traditional forecasting tools. On the Feather River, PG&E and DWR are currently using the Precipitation Runoff Modeling System (PRMS) model for streamflow forecasting (see https://wwwbrr.cr.usgs.gov/projects/SW_MoWS/PRMS.html). PRMS was developed by the US Geological Survey and primarily funded for operational use by DWR, with support from PG&E. The complete set of parameters of this model was calibrated in the mid-1990s using a combination of *a priori* expert knowledge and fit to streamflow data [31]. Now, blended hydrologic data from wireless sensor networks and remote sensing represent an innovative set of tools to support a comprehensive re-calibration using multi-objective validation. The aim of such an approach is to more closely and accurately represent the physical world with the model and, importantly, improve the model's capability of capturing the spatial distribution of internal model states such as snow melt and

evapotranspiration. Such improvements will help make PRMS more suited to prediction as the climate changes.

PRMS Recalibration Strategy

Our re-calibration strategy for PRMS is summarized in Figure 13. While the model is currently available for all sub-basins upstream of Lake Oroville, our primary focus is on the North Fork and particularly the East Branch. As discussed in Section 2.1.1, the East Branch's streamflow-generation mechanisms are largely unknown, leading to high uncertainty in streamflow forecasting at the daily, monthly, and seasonal scales. The East Branch is also representative of other, mostly ungauged catchments in the rain-snow transition zone in the Sierra Nevada, where improving forecasting skills will be critical to adequately responding to climate change.

The first step focuses on using WSN data to perform a two-part analysis of parameter sensitivity and model uncertainty in PRMS [34]. The objective is to identify the dominant parameters governing snow and streamflow response in this application and the most informative data sources and temporal periods to assign optimal parameter values. Distributed hydrologic models such as PRMS tend to rely on hundreds or thousands of parameter values, the interactions between which are often nonlinear. Sensitivity analyses identify which parameters most heavily impact model output, an important step for model recalibration. Equally importantly, addressing model's conceptual uncertainty will help identify the most relevant limitations of the model itself, namely, which physical processes are not well represented, even with optimal parameters [46].

Like all hydrologic models, PRMS indeed relies on parameterizations and simplifications of the physical processes it simulates. Such simplifications are meant to seek a trade-off between input data, computational time, and physical realism [32]; however, this approach can lead to issues of overparameterization, where optimal parameters are often impossible to estimate [10]. Another common problem is overfitting, where parameters are overtuned to past observations but not well calibrated for predictive ability. This issue is particularly common when models are calibrated only to one output, rather than to multiple metrics and variables [10]. Because PRMS has dozens of parameters, many of which are spatially distributed, and because it was originally calibrated only on streamflow, it is likely both overparameterized and overfitted. Structural uncertainty for this model is still largely unknown and unquantified. This is an issue when applying hydrologic models in forecasting mode [47], especially in view of the heavy interaction between these models and subjective choices by forecasters [45]. Further details about the methods of this step are reported in Appendix C.

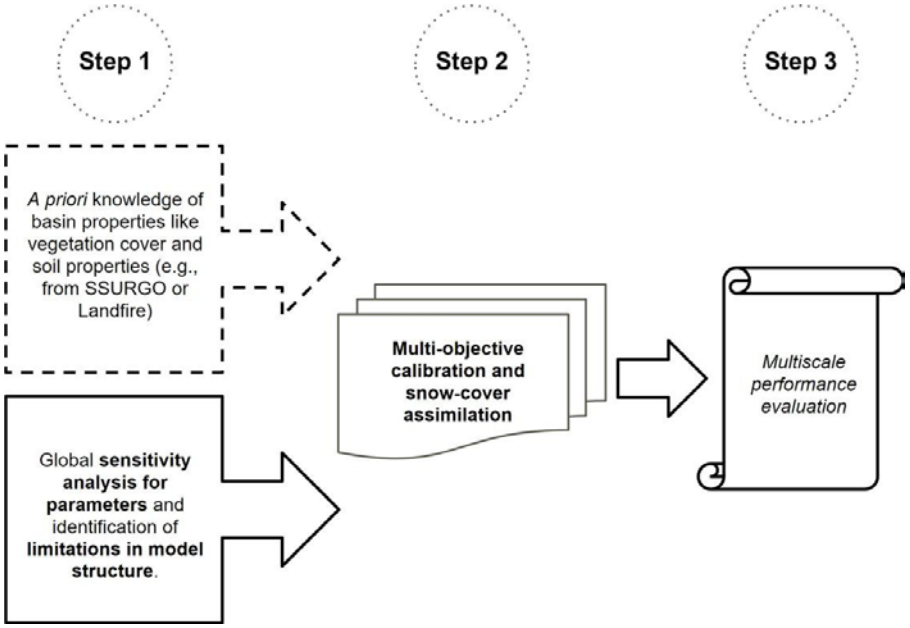

Figure 13: Proposed re-calibration strategy for PRMS on the Feather River.

This focus on parameter and model uncertainty coexists with an *a priori* knowledge of basin properties like vegetation and soil parameters [31], which are assumed the same as those assigned during the previous calibration (see the dashed box in Figure 13). PRMS reconstructs the spatial variability of the water budget by using Hydrologic Response Units (HRU), which can be idealized as portions of the catchment where hydrologic fluxes and basin properties are homogeneous. Due to both computational constraints and lack of detailed input data, existing HRUs on the Feather River are relatively large and cover broad elevation ranges. Within the East Branch, for example, the area of HRUs spans 1,100 and 13,539 acres (4.4 to 55 km^2, [31]). This spatial schema likely introduces substantial error into the model, which may in future be improved by reducing the size of each HRU. WSN data are particularly well-suited to such improvements, as they measure snow and weather variables along an elevation transect and for different canopy features, providing a detailed dataset at fine temporal resolution.

The second step of the re-calibration considers a multi-objective approach to calibrate the most meaningful parameters (Appendix C). A multi-objective method allows us to improve the physical representativeness of PRMS for intermediate model states (like SWE) while preserving performances in terms of streamflow. The ability to accurately model internal states is important to maintain an accurate understanding of the overall water balance.

This calibration step also includes assimilation of PRMS predictions with blended maps of SWE to achieve a realistic reconstruction of snow water equivalent. Previous attempts on the Feather River have shown that assimilating snow-cover patterns in a hydrologic model is not a guarantee of better performance of hydrologic models or forecasts [52]. This means that model's calibration and SWE assimilation should be conceived in an integrated framework to ensure that snow/soil/runoff parameters are physically representative rather than the result of a mere numerical fit.

The final step of the re-calibration is model validation. As mentioned, many traditional approaches, including the first PRMS calibration on the Feather River, focus on streamflow as the primary evaluation metric. Though partly due to limited data availability and computational power at the time of the original calibration, this approach can be problematic for forecasting because it results in overfitting. Thanks to both remote-sensing and ground-based data platforms (including wireless sensor networks), new targets of validation include precipitation phase, air temperature, solar radiation, SWE patterns across the landscape, annual evapotranspiration [22], soil moisture, and, of course, streamflow. Most of these fluxes are either directly measured by WSNs at 15-minute temporal resolution or easily derivable from blending WSNs with other information (see Section 3.2.2).

The improved PRMS model for the Feather River will be tested by simulating real-time forecasting conditions. Previous experience in California shows that combining traditional fore- casting techniques and dynamic models improves forecasting skills compared to the standard, statistical method employed by DWR [47]. Currently (May 2018), this step of the project is in its early stage. To set the ground for a more extensive sensitivity analysis, we have performed an initial review of available WSN data to analyze relevant hydrologic processes in the Feather River. The process we most closely focused on, given its complexity in modeling and relevance as a streamflow-generation mechanism, was rain-on-snow events (see Section 2.2). Three important sources of conceptual and calibration uncertainty related to modeling and forecasting rain-on-snow events are phase partitioning between rainfall and snowfall (when/where is it raining?), snow melt generation (when/where is the snowpack melting?), and water infiltration vs. overland flow (when/where is runoff generating?) [60].

Better understanding these processes using WSNs will support both the identification of model uncertainties and plausible ranges for each parameter that we wish to examine during the sensitivity analysis. The rain-on-snow work will therefore allow us to define these ranges based on real observations rather than making *a priori* assumptions. Our investigation of the data is described in Section 3.3.3. Included in this first assessment are additional wireless sensor networks installed in the American and Kings River of California. This choice facilitated a comparative approach to contextualize results on the Feather River from a broader perspective. More information is available in Appendix A.

3.3.2 Calibration and Conceptual Uncertainty: The Case of Rain-on-Snow

The impact of rain-on-snow events on downstream reservoirs depends on complex mass and energy processes occurring within (or around) the seasonal snow cover. These processes include interception of precipitation and wind-sheltering effects by trees [9], melt at the snow surface [60], and water flow in snow [3]. Because the Sierra Nevada is largely covered by forests and characterized by complex topography, the spatial response of snow during rain-on-snow is highly variable in space. However, this variability is generally under-captured by operational hydrologic models and has been never systematically quantified [7, 9, 38].

Figure 14 quantifies this uncertainty by showing annual Root Mean Square Errors (RMSE) for daily streamflow at the outlet of the East Branch (East Branch near Rich Bar, data from USGS and PG&E). These statistics were calculated by approximately partitioning the water year in three reference periods depending on the predominant hydrologic process: snow melt between water-year day 150 and 250 (February 27 and

June 7), precipitation between water-year day 350 and 150 (September 15 and February 27), and evapotranspiration between water-year day 250 and 350. Rain-on-snow periods were selected as days for which three-day cumulative rainfall was greater than 0.78 inches (20 mm) and average three-day snow depth was greater than 9.84 inches (25 cm). We used the standard calibration set by [31].

Results show that periods of rain-on-snow generally return higher RMSE (namely, worse performance) compared to the rest of the year. Overall, the RMSE for precipitation, snow melt, and evapotranspiration periods is equal to 1200 ft^3/s (34 m^3/s), 1270 ft^3/s (36 m^3/s), and 212 ft^3/s (6 m^3/s), respectively. RMSEs for periods of rain-on-snow is equal to 5226 ft^3/s (148 m^3/s). Rain-on-snow events also convey much more streamflow than any other period of the year: average flow during such events is equal to 7910 ft^3/s (224 m^3/s), whereas average streamflow for precipitation, snow melt, and evapotranspiration reads 741 ft^3/s (21 m^3/s), 1700 ft^3/s (48 m^3/s), and 204 ft^3/s (5.8 m^3/s), respectively.

Detecting rain-on-snow. The PRMS models uses daily minimum and maximum temperature to classify precipitation as rain or snow. As discussed in Section 3.1.4, however, WSNs can discriminate between phases by blending snow-depth and precipitation data [62]. Figure 15 compares the proportion of snowfall over total precipitation for simultaneous surface air temperatures as obtained from this blending procedure over the three basins of the Feather, American, and Kings Rivers (see Appendix A for details about the partitioning method). With data primarily collected in the rain-snow transition zone, no site converges to 100% (0%) snow even at cold (warm) temperatures. These observations could be the result of fast-moving microclimates, which can cause phase shifts on shorter timescales than air temperature changes.

Figure 16 compares hourly phase partitioning using snow-depth and rain-gauge data to the temperature partitioning thresholds used by the PRMS. PRMS compares these thresholds to daily minimum and maximum temperature values to classify precipitation. Although the observations used in this plot were hourly, Figure 16 qualitatively demonstrates that the current calibration of PRMS on the Feather River is biased towards snow events. The majority of observed mixed events would indeed be classified as snow by the model.

Impact of rain-on-snow on snowpack. We used the multi-layer physics-based snow model SNOWPACK to solve the detailed energy-mass balance of snowpack during rain-on-snow events at all the available WSNs (see Appendix A) and to identify the dominant snow melt patterns and their variability in space. Contrary to the snow module of PRMS, SNOWPACK (https://models.slf.ch/) simulates properties like density or grain size for every layer of snow, it predicts water flow through snow using Richards Equation [58], and includes a two-layer canopy module that reconstructs radiative and turbulent energy fluxes as a function of canopy parameters that are variable from tree to tree (leaf area index, fraction of throughfall, canopy height, stand basal area). These features make SNOWPACK a more detailed and realistic modeling tool to characterize rain-on-snow properties throughout the Sierras. A direct comparison between SNOWPACK and PRMS simulations will help identify major sources of modeling uncertainty in PRMS and will be the target of future research.

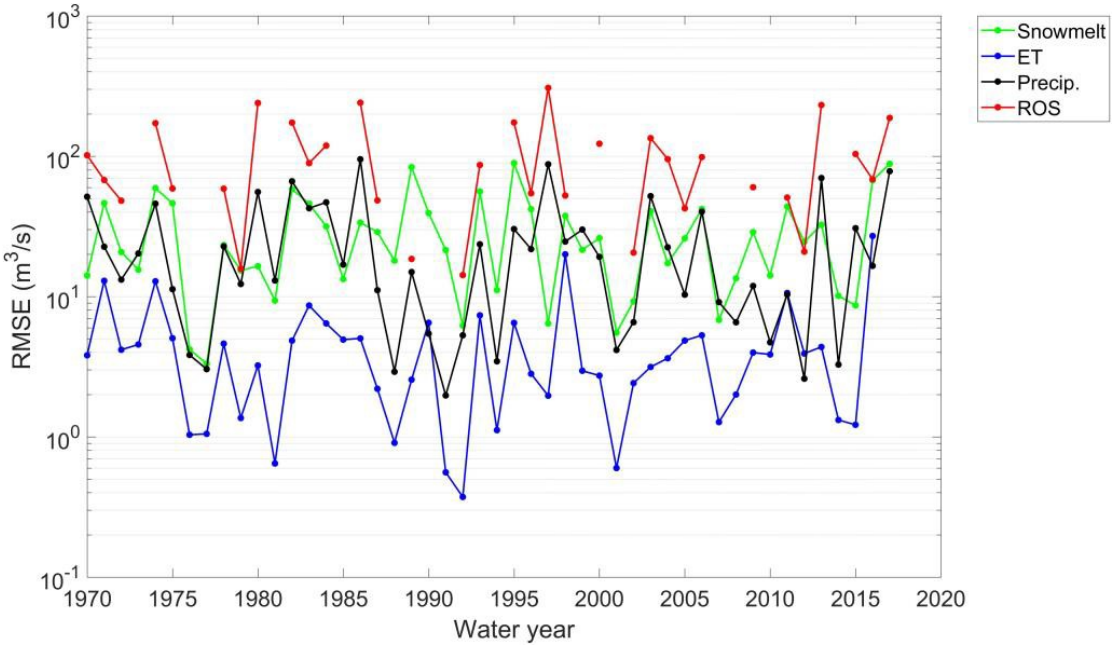

Figure 14: Annual Root Mean Square Errors (RMSE) for daily streamflow at the outlet of the East Branch for three reference periods (depending on the predominant hydrologic process, namely, precipitation, evapotranspiration, and snow melt) and rain-on-snow events (ROS). In terms of customary units, 0.1 m^3/s corresponds to 3.53 ft^3/s, 1 m^3/s corresponds to 35 ft^3/s, 100 m^3/s corresponds to 353 ft^3/s.

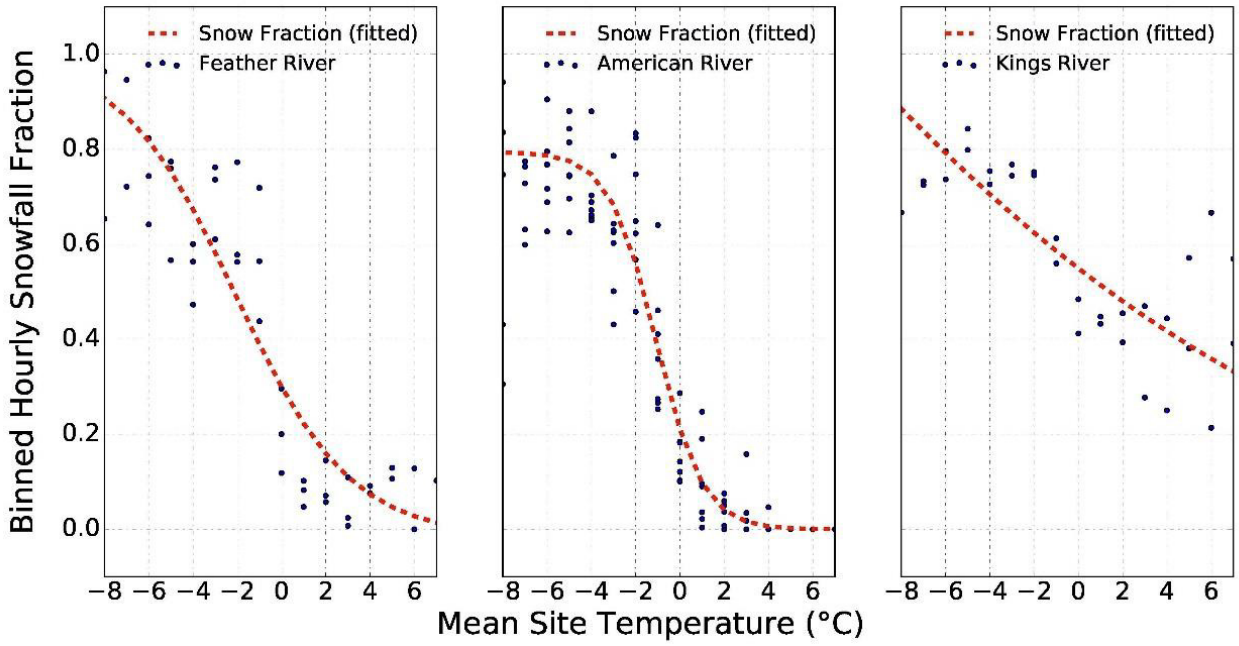

Figure 15: Proportion of precipitation that falls as snow binned by surface air temperature. -8 to 6 °C corresponds to 17.6 to 43 °F.

At all sites, rain-on-snow events are defined as any event in which, at some point during the event, at least 0.78 inches of rain (20 mm) falls within 24 hours on at least 9.85 inches (25 cm) of snow (this definition is similar to that used in Figure 14 but downscaled at hourly resolution). Technical details about SNOWPACK setup are reported in Appendix A at the end of this report. While these simulations may suffer from some uncertainties (including parameter estimation and input data availability; see Appendix A), they provide an initial framework for assessing rain-on-snow impacts on snowpack and a useful benchmark for the PRMS snow module.

Figure 17 shows an example of a rain-on-snow event that occurred at Grizzly Ridge during the Oroville incident in February 2017. As all events considered from here on, it was characterized by at least 75% of rain, average air temperature during periods of rain above 23 °F (-5 °C), and relative humidity above 80% (rain-snow partitioning performed following the same approach used in the previous paragraph). Snow depth decreased at all nodes (measured), whereas bulk snow density increased (both measured and simulated). Simulated runoff onset across the site showed marked differences, with nodes in open areas showing an earlier response than vegetated nodes. This pattern agrees with simulated time-series of volumetric bulk liquid water content in snow. The simulated lag time between the first and the last node contributing to snow melt runoff at this site was in the order of 24 to 36 hours. This difference may be attributable to differences in initial snow depth and liquid water content between nodes, which in turn depend on canopy and topography.

Figure 18 expands on this example by comparing the mean difference in snow depth and density during rain-on-snow events with the minimum - maximum difference at the same site and for the same event (results cover all the three river basins). Even though we only considered events with at least 75% of rain, about 65 (60)% of them show increasing snow depth (decreasing density), likely due to phase shifts during the storm (i.e., effect of snowfall). The variability between minimum and maximum change in snow depth and density across the same site increases in cases of overall increasing mean snow depth (or decreasing mean density), likely due to canopy interception of falling snow. Overall, the mean differences between minimum and maximum change in snow depth and density, lag time, and cumulative runoff during a rain-on-snow event at the same site are equal to 7 inches (18 cm), 62 kg/m^3 (3.9 lb/ft^3), 8.5 h, and 1.6 inches (40 mm), respectively. The spatial response of snow to rain-on-snow in the transition zone of the Sierra Nevada may therefore depend on both storm phase and canopy coverage.

Figure 19 correlates the mean incoming energy for each site and rain-on-snow event with mean net shortwave radiation, net longwave radiation, latent heat, and sensible heat at the same site (unit is mm of melt equivalent for pure ice, following [60]). These represent the most relevant energy fluxes during rain-on-snow events. Overall, (simulated) mean net longwave radiation was negative for all events, whereas other fluxes were comparable in magnitude and positive (meaning that they represented a net gain of energy for the snowpack). The values of these fluxes suggest that radiative and turbulent energy fluxes may provide a comparable, overall contribution to melt during rain-on-snow in vegetated areas like the Sierra Nevada. This result highlights the importance of both canopy-snow interactions and wind-sheltering effects in hydrologic models. However, total incoming energy was highly correlated with both latent and sensible fluxes (coefficient of determination $r^2 = 0.83$ and 0.89, respectively), whereas $r^2 = 0$ for both net shortwave and

longwave radiation. These results agree with previous findings by [60] and suggest that wind could be an important driver of melt during greater rain-on-snow events (especially on the Feather River and water year 2017). Currently, wind speed is not used as an input data of PRMS; future development steps could consider including this addition to try to improve its performance during intense rain- on-snow events.

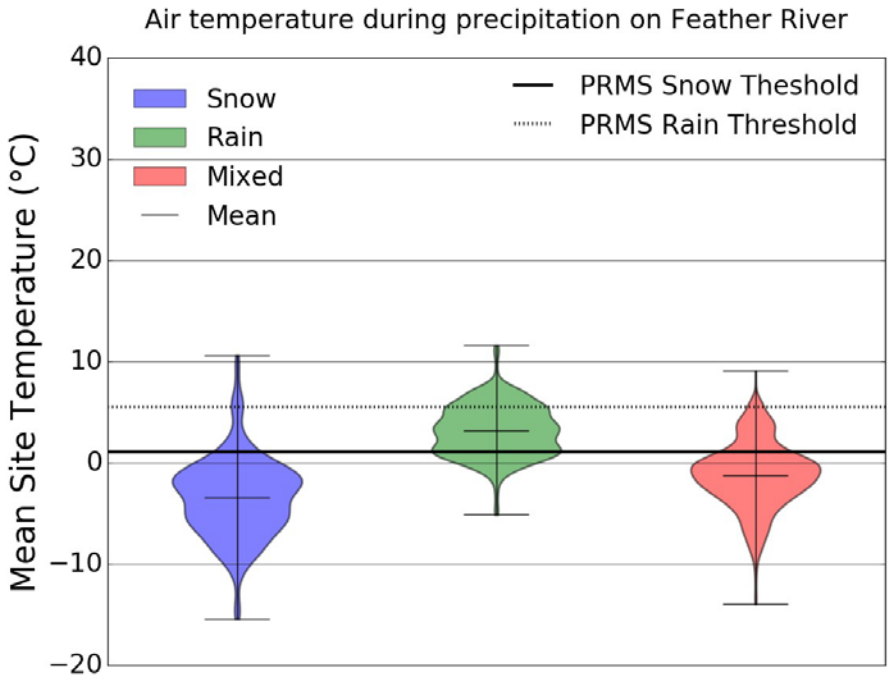

Figure 16: Temperature of precipitation hours as observed on the three sites on the Feather River vs. temperature partitioning thresholds used by the PRMS. -15 to 40 °C corresponds to 5 to 104 °F.

Impact of rain-on-snow on soil-water storage: Figure 20 compares soil-water storage response to rain-on-snow events (red highlights) at sites in the Feather (left-hand panel) and Kings River basins (right-hand panel, see Appendix A for the technical details about how water storage was estimated). In the 2008-2016 record at Kings River sites, deeper snow reduces soil-water storage variability during rain-on-snow events. In contrast, during the extreme precipitation events in the Feather River basin during 2017, there is greater soil-water storage variability irrespective of snow depth. These deviations translate into large scatter in the first derivative of soil-water content for any snow depth (Figure 21, right panel), as opposed to the Kings River. No detailed information about snow and/or soil properties is available at these sites to potentially relate this difference to geology or snow properties. One hypothesis is that the greater soil-water storage variability in the Feather may be due to increased grain size and/or preferential channels due to larger precipitation events, making the snowpack prone to deeper percolation of water irrespective of snow depth [4]. This discrepancy could also be related to differing predominant geological properties between the two basins, as the Feather River straddles the transition between the granitic Sierra Nevada and

the volcanic southern Cascade Range while Kings River geology is purely granitic. In any case, snow depth, snow stratigraphy, and precipitation regime affect soil-water storage during rain on snow. Soil moisture sensors can potentially assist forecasters with timely insight into the fate of precipitation and snowmelt at local scale.

Key findings and lessons learned: The key findings of this focus on rain-on-snow on the Feather River are that:

1. Models that rely on temperature indexing for phase partitioning should use a wider temperature range for mixed rain-snow events. In particular, the temperature threshold where all precipitation is classified as snow should be lower (Figure 16).
2. Wireless sensor networks, in contrast to single, point stations, can capture significant variability in mass and energy fluxes of snow during rain-on-snow events at the WSN scale (Figures 17 and 18).
3. Radiative and turbulent energy fluxes seem comparable for most events due to possible sheltering effect of canopy. The total energy input seems highly correlated with turbulent fluxes, which in turn depend on wind speed and air temperature (Figure 19).
4. Snow depth, snow stratigraphy, and precipitation regime affect soil-water storage during rain on snow. Models are needed which can accurately model preferential flow of water through snow to adequately simulate mid-winter storage changes (Figure 20).

Public authorities, utility companies, and water agencies, including DWR and PG&E, forecast streamflow and water incoming volume at reservoirs for different temporal scales, from seasonal to daily. The streamflow response of rain-on-snow events occurs at a relatively short temporal scale (say, up to a few days). However, this time scale dramatically depends on infiltration vs. surface-runoff patterns for different slopes and subbasins. Also, the spatial distribution of snow cover and SWE after rain-on-snow events can affect bulk SWE and snow depth, which are routinely used by forecasters in statistical relationships with precipitation and seasonal water volume [47]. Better capturing the phase of precipitation and the response of snow and soil during rain-on-snow events will allow forecasters to (1) improve delineation of basin areas where rain (snow) is occurring, namely, where runoff response is expected to be fast (slow), (2) estimate the difference in SWE between standard, index stations and areas with different canopy/slope (so-called depletion rate). These results will, therefore, provide the basis for better modeling and forecasting at basin scale.

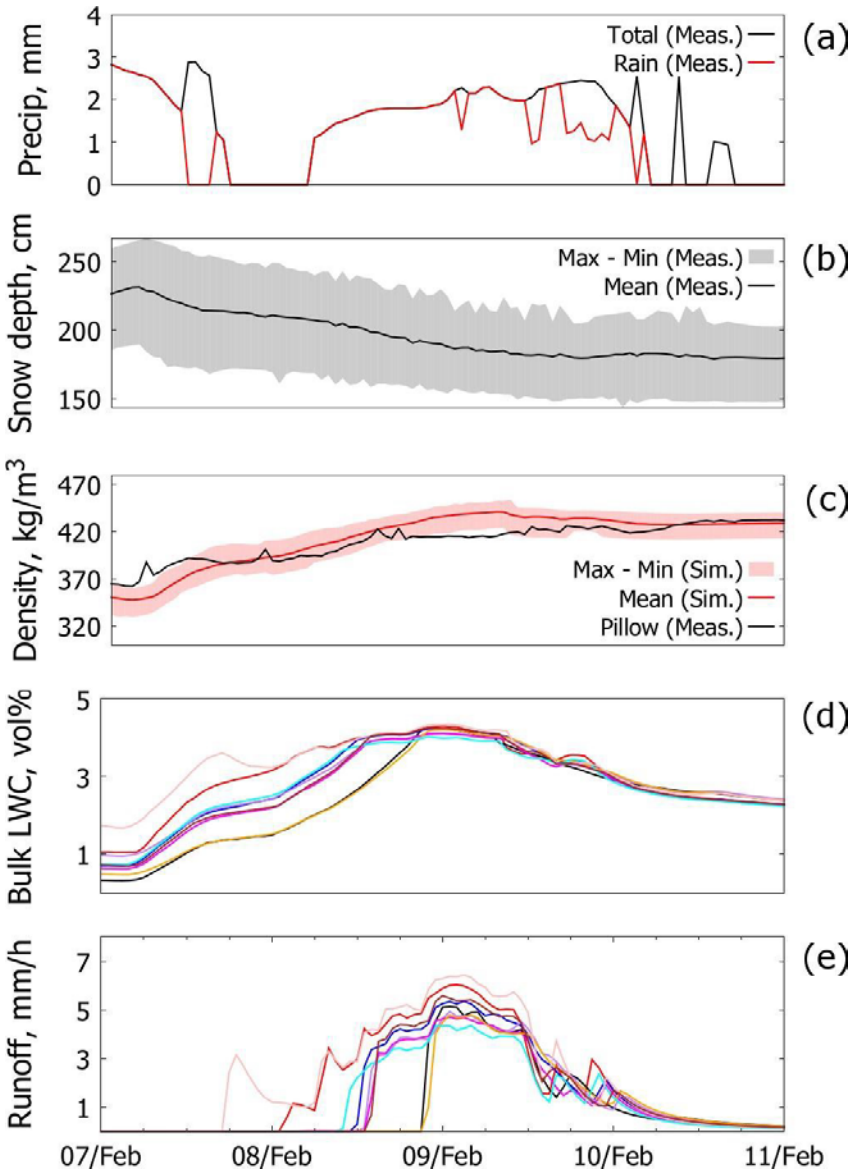

Figure 17: Snow response to the February 2017 rain-on-snow event in Grizzly Ridge (Feather River, same period of the Oroville incident). In panel (d) and (e), different colors are different nodes across the site (both results are outputs of the SNOWPACK model). Ranges in customary units are as follows: 0 to 4 mm corresponds to 0 to 0.15 inches (a), 150 and 250 cm corresponds to 60 to 98 inches (b), 1 to 7 mm/h corresponds to 0.04 to 0.27 inches/hour (e).

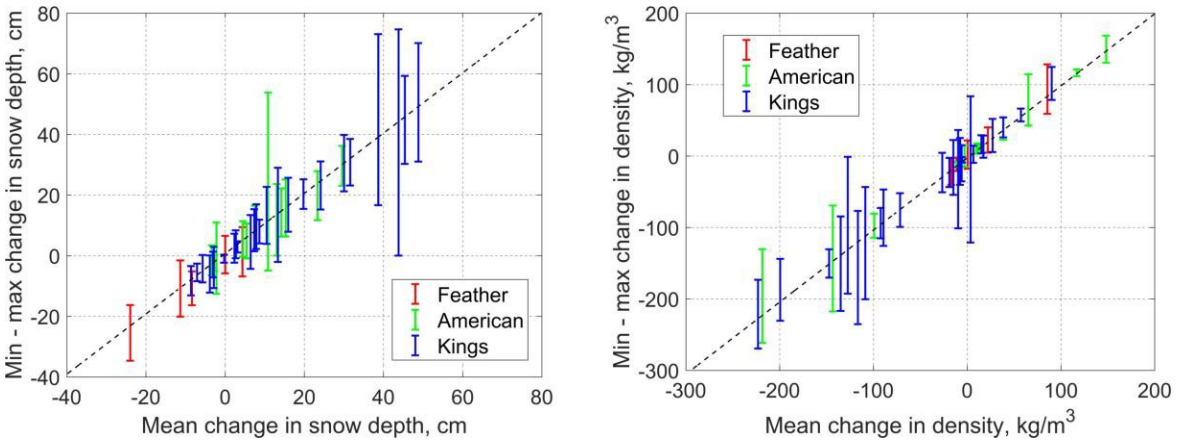

Figure 18: Change in snow depth and density during rain-on-snow events. Each bar represents a different event and site. - 40 to 80 cm corresponds to -15.7 to 31.5 inches on the first subplot; -300 to 200 kg/m^3 corresponds to -18.7 to 12.5 lb/ft^3 on the second subplot.

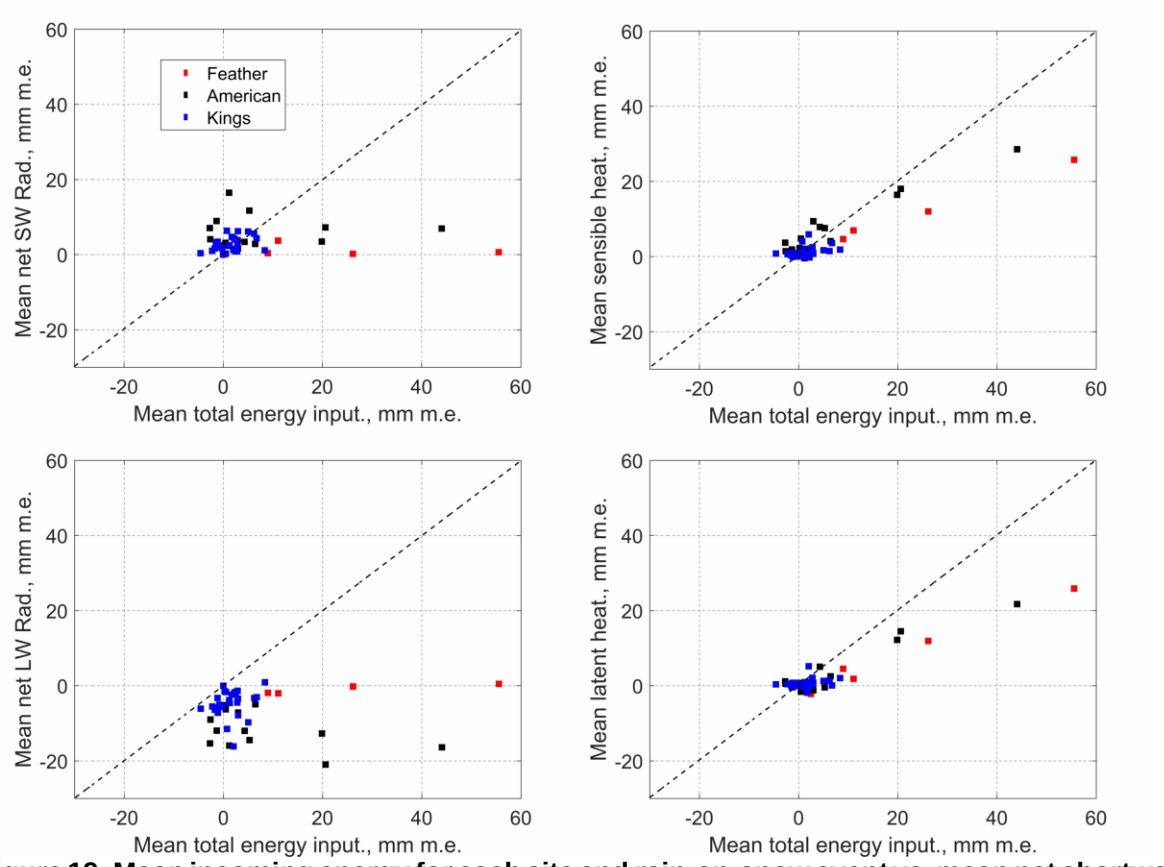

Figure 19: Mean incoming energy for each site and rain-on-snow event vs. mean net shortwave radiation, net longwave radiation, latent heat, and sensible heat for the same site and event (unit is mm of melt equivalent for pure ice). - 30 to 60 mm corresponds to -1.18 to 2.36 inches.

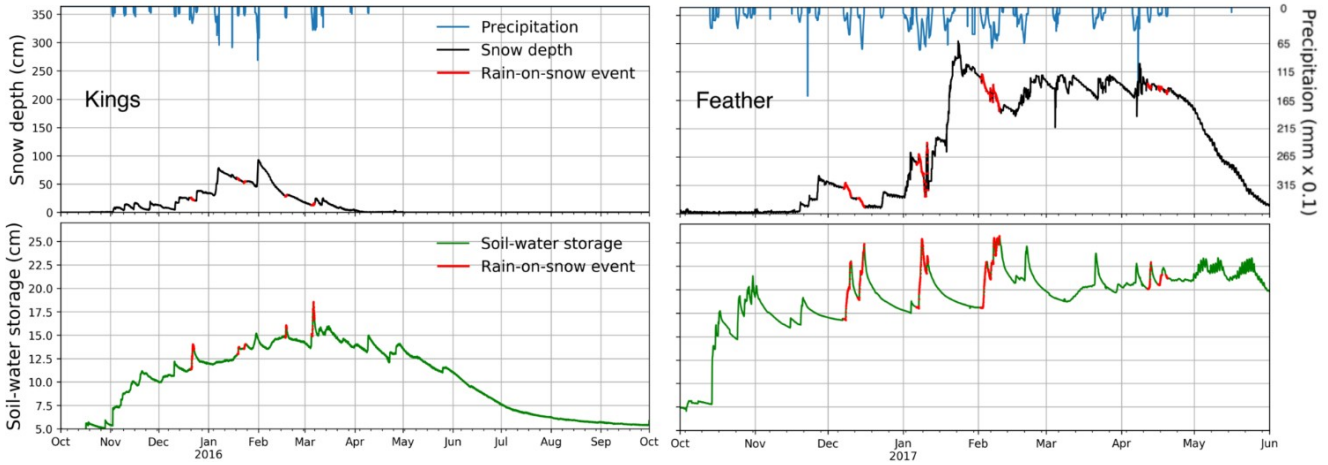

Figure 20: Soil-water storage response to rain-on-snow events (red highlights) at sites in the Kings (left-hand panel) and Feather River basins (right-hand panel). 350 and 25 cm correspond to 138 and 10 inches, respectively.

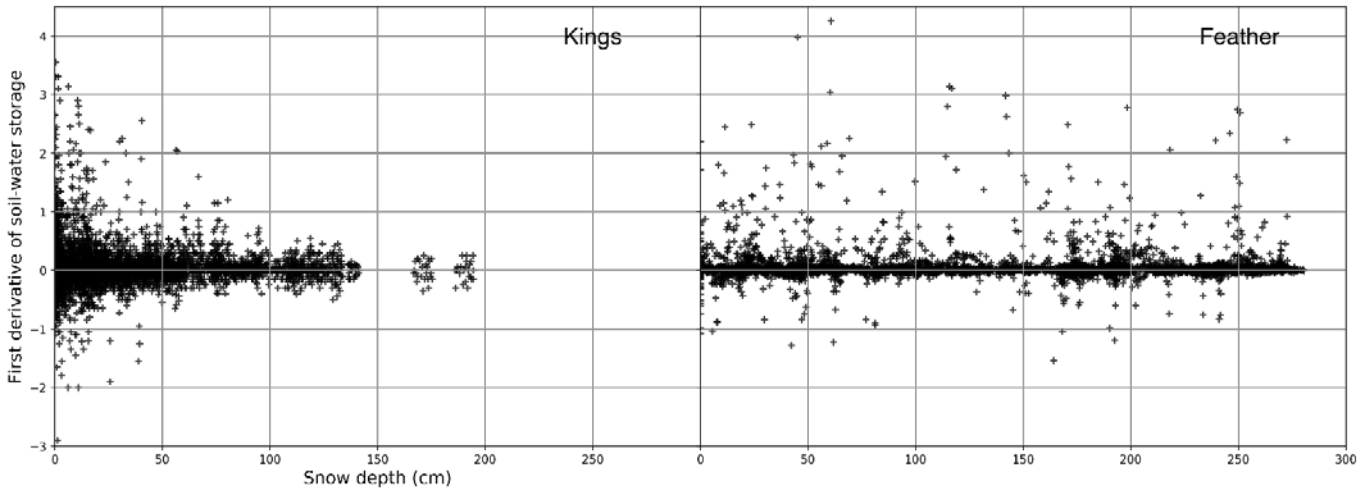

Figure 21: Change in soil storage by snow depth in the Kings and Feather River basins. The Kings River shows a clear threshold of snow depth above which soil storage is not affected. This is not true on the Feather. 0 to 300 cm corresponds to 0 to 188 inches.

4: Conclusion and Future Directions

4.1 Objectives and Current Progress

The objectives of the Feather River Hydrologic Observatory (FRHO) are to:

1. Create an intelligent water-information system to optimize real-time knowledge of hydrology across the landscape.
2. Use this system to provide more detailed water-basin storage information.
3. Leverage this advanced monitoring capability to improve current runoff predictions and forecasting on the North Fork of the Feather River.
4. Demonstrate the actual cost savings from using this decision-support chain for Feather River stakeholders, including utility companies and water agencies.
5. Ultimately, contribute to reducing the effects of climate change on California hydropower generation.

The project team has installed four wireless sensor networks (WSNs) that collectively comprise a state-of-the-art water information system. This system will help improve understanding of the hydrologic processes that govern streamflow generation (objective 1), including precipitation phase, snow water equivalent (SWE) distribution, and soil moisture patterns under a variety of landscape features and events such as rain-on-snow. An examination of the first year of available data on the Feather River (water year 2017) has shed light on these processes and the limitations of current modeling tools (objective 2). In addition, maps are being created to show the distribution of SWE across the landscape. The project team has begun work for a sensitivity analysis of the Precipitation Runoff Modeling System (PRMS), which is the first step toward a recalibration of the model in hopes of improving streamflow predictions (objective 3). Objectives 4 and 5 will be addressed in the coming months.

The findings from the first year of data collection and analysis have yielded several promising results. Firstly, the WSNs have demonstrated value as resilient and consistent tools for data collection even in harsh montane conditions. Despite the 2017 water year being one of the wettest on record in the northern Sierra Nevada, the networks remained largely functional and were able to consistently deliver real-time data [36]. This represents a promising result in terms of network reliability for the next years of the project and future deployments in other locations.

A review of the data from the 2017 water year confirmed expectations that traditional sensing stations, such as snow pillows, generally give biased pictures of snowpack conditions in mountains. When compared with the mean of the WSN readings, manual snow courses and snow-pillow locations generally show greater snow depth and a later melt-out date. These differences are likely due to traditional stations' locations in flat, open meadows, which do not capture varying conditions under canopy and on slopes as the WSNs do. Moreover, additional measurements taken by the WSNs, such as relative humidity, solar radiation, and soil moisture, allow more components of the water balance and additional hydrologic processes to be examined. Blending point data from snow pillows and WSNs with remote-sensing products can successfully provide daily maps of SWE for the whole Feather River. Initial results show promise in being able to replicate

snow accumulation and ablation patterns, which can greatly increase forecasting abilities, particularly during the snow melt season. Accurate blended maps will also facilitate a re-calibration of PRMS, where SWE estimates can be assimilated into the model to correct internal state variables.

An initial data review, focusing particularly on rain-on-snow events, revealed possible limitations of the PRMS model and gave an indication of appropriate parameter ranges to explore during the planned sensitivity analysis. In particular, a rain-snow partitioning method based on blending WSN data with existing rain gauges demonstrated that the partitioning system used by PRMS, which is based on daily minimum and maximum temperature, is likely overestimating the proportion of precipitation that falls as snow. Since rain generates streamflow on far different time scales than snow, this distinction is important.

Furthermore, the data review revealed an inconsistent response of snowpack properties to rain-on-snow events. For example, on average, some rain-on-snow events decreased snow depth across the site, while others increased snow depth due to mixed precipitation types during the storm. Events that increased snow depth generally showed greater spatial variability across the sites since canopy interception affects snow distribution more than rain. Using the one-dimensional point model SNOWPACK with WSN data as inputs also suggests a significant variability in runoff generation across nodes.

Finally, the rain-on-snow events showed mostly consistent response to soil moisture, where higher snow depths were correlated with little-to-no change in soil moisture. The exception was the Bucks Lake site on the Feather River during the 2017 water year, where storms had a significant impact on soil storage irrespective of snow depth. This finding suggests the need for improved modeling tools that can jointly simulate water movement through snow and soil.

4.2 Future Directions

The next major step will be a recalibration of PRMS beginning with a generalized sensitivity analysis. This step aims to identify the optimal baseline parameters for the model while simultaneously diagnosing sources of model bias. This work will help quantify the different sources of uncertainty inherent in a model, such as parameter identification or structural model bias. As part of the recalibration, the team will investigate the use of the blended SWE maps that are being finalized. The goal is to assimilate the SWE maps into the PRMS model as it runs, allowing internal model states to be updated based on simultaneous observations. As noted in Section 3.3.2, assimilation must be performed jointly with recalibration to maximize the chances of improving hydrologic forecasts.

As part of this work, the data from the wireless sensor networks will be incorporated into existing decision-support systems for forecasting on the Feather River. The outputs of this project—that is, real-time temperature, snow, and soil-water storage data from wireless sensor networks, blended SWE maps at basin scale, and improved streamflow predictions from PRMS – will allow forecasters to perform continuous reality checks between forecasting tools and ground-based/remote-sensing data. This system will pave the way to more adaptive decision-support tools (particularly helpful in light of a changing climate) while allowing users to make quick, manual changes to the most important parameters

when forecasting. In this way, forecasting tools will leverage expert knowledge and state-of-the-art data collection to address specific situations.

The final major step will be an economic assessment of this updated PRMS tool to determine the cost savings achieved by improved forecasting. A cost-benefit analysis will then be performed to determine the net impact of the wireless sensor networks.

4.3 Relevance for Climate Change-Related Policy and Decision Makers

From a hydroelectricity standpoint, the potential impacts of this project reach beyond PG&E and even California. In the context of climate change, improving streamflow forecasting will be particularly important for reducing risks for utilities and controlling prices for ratepayers. The first and most direct reason is that climate change is projected to alter precipitation patterns across the Sierra Nevada. A greater proportion of precipitation is projected to fall as rain rather than snow, which will reduce snowpack and change the timing of seasonal flow. Recent evaluations of water-supply forecasts in California show that forecast skills increase with the average elevation of the target basin [75], reflecting increased uncertainty in rain-dominated catchments at lower elevations compared to snow-dominated regions. A climate-change-induced transition from snow to rain could therefore result in more uncertain seasonal forecasts at downstream powerhouses [51]. Since many powerhouses in California, including most on the Feather River, do not have substantial storage facilities, streamflow predictions are crucial to making informed operational decisions.

A more indirect effect, related to energy prices on the open market, is already being felt by utility companies. California, like many other states, has ambitious goals for the integration of variable generation such as wind and solar into the electric grid. Renewable Portfolio Standards (RPS) have contributed to a growing mismatch at certain hours of the day between available energy and demand. During the afternoons, abundance of solar and wind energy may contribute excess energy to the grid, lowering the prices for all energy sources. If prices fall below the cost of production, hydropower (or any other energy source) becomes a net profit loser, posing difficulties for utility companies. Accurate streamflow forecasts may help keep hydropower plants economical even with greater changes in energy markets and climate.

Despite the focus on streamflow forecasting for hydroelectricity production, the project also has broader implications related to water resources and flood control. As the spillway damage at Oroville Dam demonstrated in February 2017, the impacts of certain types of events, like rain-on-snow, on California's water system are not well understood or predictable. Because Lake Oroville is the primary supply of water for the State Water Project, which delivers water to many major cities of Southern California, the incident affected water supply and flood control. WSNs have the potential to improve forecasting for both by better informing our understanding of such hydrologic processes. If rain-on-snow events become more common due to climate change, these forecasts will be all the more important.

The ability to improve forecasting may help with water supply management both in California and across the United States. The effect of climate change on total precipitation rates in California is uncertain [24], but whether they increase or decrease, careful management of water systems to maximize water availability or minimize flood risk will

be necessary. Improved forecasting tools will help water utilities make operational decisions under such circumstances.

A final point should be made concerning the value of this cross-disciplinary project. Bringing together public agencies (such as the Energy Commission and DWR), California's largest energy utility (PG&E), and multiple campuses of California's public university system (Berkeley and Merced), the project shows the value of collaboration among multiple entities. It also demonstrates the direct applicability of hydrologic and sensors research to address practical problems and helps to bridge the gap between theoretical research and the on-the-ground challenges that utility operators, at PG&E and across the state, face on a daily basis.

5: References

[1] E. A. Anderson. A Point Energy and Mass Balance Model of a Snow Cover. Technical report, NOAA Technical Report NWS 19, 1976.

[2] Associated Press. Oroville Dam Spillway Repair Costs to Top $500M, Doubling Initial Estimate. 2017. https://www.nbclosangeles.com/news/california/Oroville-Dam-Repair-Costs-California- Flood-Storm-451903223.html. Accessed 30 October 2017.

[3] F. Avanzi, H. Hirashima, S. Yamaguchi, T. Katsushima, and C. De Michele. Observations of capillary barriers and preferential flow in layered snow during cold laboratory experiments. The Cryosphere, 10(5):2013 - 2026, 2016.

[4] F. Avanzi, G. Petrucci, M. Matzl, M. Schneebeli, and C. De Michele. Early formation of preferential flow in a homogeneous snowpack observed by micro-CT. Water Resources Research, 53(5):3713–3729, 2017.

[5] R. Bales, N. P. Molotch, T. H. Painter, M. D. Dettinger, R. Rice, and J. Dozier. Mountain hydrology of the western United States. Water Resources Research, 42:W08432, 2006.

[6] P. Bartelt and M. Lehning. A physical snowpack model for the Swiss Avalanche Warning: Part I: numerical model. Cold Regions Science and Technology, 35(3):123 – 145, 2002.

[7] N. Berg, R. Osterhuber, and J. Bergman. Rain-induced outflow from deep snowpacks in the Central Sierra Nevada, California. Hydrological Sciences Journal, 36(6):611–629, 1991.

[8] W. R. Berghuijs, R. A. Woods, and M. Hrachowitz. A precipitation shift from snow towards rain leads to a decrease in streamflow. Nature Climate Change, 4:583 – 586, 2014.

[9] S. N. Berris and R. D. Harr. Comparative snow accumulation and melt during rainfall in forested and clear-cut plots in the Western Cascades of Oregon. Water Resources Research, 23(1):135–142, 1987.

[10] K. Beven. A manifesto for the equifinality thesis. Journal of Hydrology, 320(1):18 – 36, 2006.

[11] California Department of Water Resources. "Climate Change." 2017. http://www.water.ca.gov/climatechange/. Accessed 24 October 2017.

[12] California Energy Commission. Total System Electric Generation, 2013-2015. 2017. http://www.energy.ca.gov/almanac/electricity/data/system/power/2015/total/system/power.html. Accessed 24 October 2017.

[13] D. R. Cayan, E. P. Maurer, M. D. Dettinger, M. Tyree, and K. Hayhoe. Climate change scenarios for the California region. Climatic Change, 87(1):21–42, Mar 2008.

[14] F. Counillon and L. Bertino. Ensemble optimal interpolation: multivariate properties in the Gulf of Mexico. Tellus A, 61(2):296–308, 2009.

[15] L.M. Cox, L.D. Bartee, A.G. Crook, P.E. Farnes, and J.L. Smith. The care and feeding of snow pillows. In Proceedings of the 46th Annual Western Snow Conference, pages 40–47, Otter Rock, Oregon, 1978.

[16] A. Dai. Drought under global warming: a review. Wiley Interdisciplinary Reviews: Climate Change, 2(1):45–65, 2011.

[17] A. J. Dietz, C. Kuenzer, U. Gessner, and S. Dech. Remote sensing of snow - a review of available methods. International Journal of Remote Sensing, 33(13):4094 – 4134, 2012.

[18] Q. Y. Duan, V. K. Gupta, and S. Sorooshian. Shuffled complex evolution approach for effective and efficient global minimization. Journal of Optimization Theory and Applications, 76(3):501–521, Mar 1993.

[19] Q. Duan, S. Sorooshian, and V. K. Gupta. Optimal use of the SWE-UA global optimization method for calibrating watershed models. Journal of Hydrology, 158(3):265 – 284,1994.

[20] M. Durand, N. P. Molotch, and S. A. Margulis. A Bayesian approach to snow water equivalent reconstruction. Journal of Geophysical Research: Atmospheres, 113(D20), 2008.

[21] G. J. Freeman. Climate change and the changing water balance for California's North Fork Feather River. In Proceedings of the 79th Annual Western Snow Conference, pages 71 – 82, Stateline, Nevada, 2011.

[22] M. L. Goulden, R. G. Anderson, R. C. Bales, A. E. Kelly, M. Meadows, and G. C. Winston. Evapotranspiration along an elevation gradient in California's Sierra Nevada. Journal of Geophysical Research: Biogeosciences, 117(G3), 2012.

[23] I. Gouttevin, M. Lehning, T. Jonas, D. Gustafsson, and M. Mölder. A two-layer canopy model with thermal inertia for an improved snowpack energy balance below needleleaf forest (model SNOWPACK, version 3.2.1, revision 741). Geoscientific Model Development, 8(8):2379–2398, 2015.

[24] E. Hanak, J. Lund, A. Dinar, B. Gray, R. Howitt, J. Mount, P. Moyle, and B. Thompson. Managing California's Water: From Conflict to Reconciliation. Public Policy Institute of California, San Francisco, 0211.

[25] B. J. Hatchett, B. Daudert, C. B. Garner, N. S. Oakley, A. E. Putnam, and A. B. White. Winter Snow Level Rise in the Northern Sierra Nevada from 2008 to 2017. Water, 9(1):899, 2017.

[26] L. E. Hay, G. H. Leavesley, M. P. Clark, S. L. Markstrom, R. J. Viger, and M. Umemoto. Step wise, multiple objective calibration of a hydrologic model for a snowmelt dominated basin. JAWRA Journal of the American Water Resources Association, 42(4):877–890, 2006.

[27] L. E. Hay and M. Umemoto. Multiple-Objective Stepwise Calibration Using Luca. Technical report, U.S.Geological Survey Open-File Report 2006-1323, 2006.

[28] K. Hayhoe, D. Cayan, C. B Field, P. C Frumhoff, E. P Maurer, N. L Miller, S. C Moser, S. H Schneider, K. Nicholas Cahill, E. E Cleland, et al. Emissions pathways, climate change, and impacts on California. Proceedings of the National Academy of Sciences of the United States of America, 101(34):12422–12427, 2004.

[29] California ISO. What the duck curve tells us about managing a green grid. Pages 1–4, 2016.
https://www.caiso.com/Documents/FlexibleResourcesHelpRenewables_FastFacts.pdf. Accessed 28 December 2017.

[30] G. Klein, M. Krebs, V. Hall, T. O'Brien, and B.B. Blevins. *California's Water-Energy Relationship*. California Energy Commission. CEC-700-2005-011-SF. 2005.

[31] K. M. Koczot, A. E. Jeton, B. McGurk, and M. D. Dettinger. Precipitation-Runoff Processes in the Feather River Basin, Northeastern California, with Prospects for Streamflow Predictability, Water Years 1971-1997. Scientific Investigations Report 5202, USGS, 2004.

[32] V. Krysanova, D.-I. Müller-Wohlfeil, and A. Becker. Development and test of a spatially distributed hydrological/water quality model for mesoscale watersheds. Ecological Modelling, 106(2):261 – 289, 1998.

[33] J. M. Lenihan, R. Drapek, D. Bachelet, and R. P. Neilson. Climate change effects on vegetation distribution, carbon, and fire in California. Ecological Applications, 13(6):1667–1681, 2003.

[34] B. F. Lund and B. A. Foss. Parameter ranking by orthogonalization—Applied to nonlinear mechanistic models. Automatica, 44:278–281, 2008.

[35] J. D. Lundquist and F. Lott. Using Inexpensive Temperature Sensors to Monitor the Duration and Heterogeneity of Snow-covered Areas. Water Resources Research, 44(4), 2008.

[36] S. A. Malek, F. Avanzi, K. Brun-Laguna, T. Maurer, C. A. Oroza, P. C. Hartsough, T. Watteyne, and S. D. Glaser. Real-time alpine measurement system using wireless sensor networks. Sensors, 17(2583), 2017.

[37] S. A. Margulis, G. Cortes, M. Girotto, and M. Durand. A LANDSAT-era Sierra Nevada snow reanalysis (1985–2015). Journal of Hydrometeorology, 17(4):1203–1221, 2016.

[38] D. Marks, J. Kimball, D. Tingey, and T. Link. The sensitivity of snowmelt processes to climate conditions and forest cover during rain-on-snow: a case study of the 1996 Pacific Northwest flood. Hydrological Processes, 12(10-11):1569–1587, 1998.

[39] S.L. Markstrom, R.S. Regan, L.E. Hay, R.J. Viger, R.M.T. Webb, R.A. Payn, and J.H. LaFontaine. PRMS-IV, the Precipitation-Runoff Modeling System, version 4: U.S. Technical report, NOAA Technical Report NWS 19 U.S. Geological Survey Techniques and Methods, 2015.

[40] N. L. Miller, K. E. Bashford, and E. Strem. Potential impacts of climate change on California hydrology. JAWRA Journal of the American Water Resources Association, 39(4):771–784, 2003.

[41] P. C. D. Milly, J. Betancourt, M. Falkenmark, R. M. Hirsch, Z. W. Kundzewicz, D. P. Lettenmaier, and R. J. Stouffer. Stationarity is dead: Whither water management? Science, 319(5863):573–574, 2008.

[42] P. B Moyle, J. D Kiernan, P. K Crain, and R. M Quinones. Climate change vulnerability of native and alien freshwater fishes of California: a systematic assessment approach. PLoS One, 8(5):e63883, 2013.

[43] State of California Legislative Counsel Bureau. Senate Bill No. 350. 48 pages. 2015. http://leginfo.legislature.ca.gov/faces/billNavClient.xhtml?bill/id=201520160SB350.

[44] C. A. Oroza, Z. Zheng, S. D. Glaser, D. Tuia, and Roger C. Bales. Optimizing Embedded Sensor Network Design for Catchment-scale Snow-depth Estimation Using LiDAR and Machine Learning. Water Resources Research, 52(10):8174–8189, 2016.

[45] T. C. Pagano, F. Pappenberger, A. W. Wood, M.-H. Ramos, A. Persson, and B. Anderson. Automation and human expertise in operational river forecasting. Wiley Interdisciplinary Reviews: Water, 3(5):692–705, 2016.

[46] J. Christian Refsgaard, J. P. van der Sluijs, J. Brown, and P. van der Keur. A framework for dealing with uncertainty due to model structure error. Advances in Water Resources, 29(11):1586 – 1597, 2006.

[47] E. A. Rosenberg, A. W. Wood, and A. C. Steinemann. Statistical applications of physically based hydrologic models to seasonal streamflow forecasts. Water Resources Research, 47(3), 2011.

[48] C. Santın, H. D. Stefan, L. Otero Xose, and C. J. Chafer. Quantity, composition and water contamination potential of ash produced under different wildfire severities. Environmental Research, 142(Supplement C):297 – 308, 2015.

[49] Sierra Nevada Conservancy. “California’s Primary Watershed.” 2011. http://www.sierranevada.ca.gov/our-region/ca-primary-watershed. Accessed 24 October 2017.

[50] E. A Stene. "The Central Valley Project." U.S. Bureau of Reclamation. 2015. https://www.usbr.gov/history/cvpintro.html. Accessed 24 October 2017.

[51] I. T. Stewart, D. R. Cayan, and M. D. Dettinger. Changes toward earlier streamflow timing across western North America. Journal of Climate, 18(8):1136–1155, 2005.

[52] Q. Tang and D. P. Lettenmaier. Use of satellite snow-cover data for streamflow prediction in the Feather River basin, California. International Journal of Remote Sensing, 31(14):3745–3762, 2010.

[53] M. TH Van Vliet, J. R Yearsley, F. Ludwig, Stefan Vögele, D. P Lettenmaier, and P. Kabat. Vulnerability of US and European electricity supply to climate change. Nature Climate Change, 2(9):676–681, 2012.

[54] S. Vicuna, R. Leonardson, M. W. Hanemann, L. L. Dale, and J. A. Dracup. Climate change impacts on high elevation hydropower generation in California's Sierra Nevada: a case study in the Upper American River. Climatic Change, 87(1):123–137, Mar 2008.

[55] S. Vicuna, E. P. Maurer, B. Joyce, J. A. Dracup, and D. Purkey. The sensitivity of California water resources to climate change scenarios. JAWRA Journal of the American Water Resources Association, 43(2):482–498, 2007.

[56] M. Weiser. Water Deeply: Why Hydroelectric Utilities Are Endangered by Soaring Solar and Wind. Nov 2017. https://www.newsdeeply.com/water/articles/2017/11/06/why-hydroelectric-utilities-are-endangered-by-soaring-solar-and-wind. Accessed 28 December 2017.

[57] N. Wever, F. Comola, M. Bavay, and M. Lehning. Simulating the influence of snow surface processes on soil moisture dynamics and streamflow generation in an alpine catchment. Hydrology and Earth System Sciences, 21(8):4053–4071, 2017.

[58] N. Wever, C. Fierz, C. Mitterer, H. Hirashima, and M. Lehning. Solving Richards equation for snow improves snowpack meltwater runoff estimations in detailed multi-layer snowpack model. The Cryosphere, 8(1):257–274, 2014.

[59] I. White, A. Wade, M. Worthy, N. Mueller, T. Daniell, and R. Wasson. The vulnerability of water supply catchments to bushfires: impacts of the January 2003

wildfires on the Australian capital territory. Australasian Journal of Water Resources, 10(2):179–194, 2006.

[60] S. Würzer, T. Jonas, N. Wever, and M. Lehning. Influence of initial snowpack properties on runoff formation during rain-on-snow events. Journal of Hydrometeorology, 17(6):1801–1815, 2016.

[61] Z. Zhang, S. D. Glaser, R. C. Bales, M. Conklin, R. Rice, and D. G. Marks. Technical report: The design and evaluation of a basin-scale wireless sensor network for mountain hydrology. Water Resources Research, 53, 2017.

[62] Z. Zhang, S. D. Glaser, R. C. Bales, M. Conklin, R. Rice, and D. Marks. Insights into Mountain Precipitation and Snowpack from a Basin-scale Wireless Sensor Network. Water Resources Research, 53, 2017.

[63] Z. Zheng, N. P. Molotch, C. A. Oroza, M. Conklin, and R. Bales. Spatial snow estimation for mountainous areas using wireless sensor networks and remote-sensing products. Submitted, 2018.

[64] United States Geological Survey. "Current Land Subsidence in the San Joaquin Valley." California Water Science Center. 18 July 2017. https://ca.water.usgs.gov/projects/central- valley/land-subsidence-san-joaquin-valley.html. Accessed 28 December 2017.

[65] State of California. "Hydroelectric Power in California." California Energy Commission. 2017. http://www.energy.ca.gov/hydroelectric/. Accessed 28 December 2017.

[66] Pacific Gas & Electric. "Learn about our hydroelectric system". 2017. https://www.pge.com/en_US/safety/how-the-system-works/hydroelectric-system/hydroelectric- system.page. Accessed 28 December 2017.

[67] Serna, Joseph. "The Kings River flooded from snowmelt that couldn't be measured or predicted." *The Los Angeles Times*. 26 June 2017. Online. http://www.latimes.com/local/lanow/la-me-ln-kings-river- flooding-snowpack-20170626-story.html. Accessed 28 December 2017.

[68] State of California. Upper North Fork Feather River Hydroelectric Project, FERC #2105. California Environmental Protection Agency: State Water Resources

Control Board. 2017. https://www.waterboards.ca.gov/waterrights/water_issues/programs/water_quality_cert/unffr_ferc2105_ eir.shtml. Accessed 28 December 2017.

[69] California Department of Water Resources. "Snowpack Shows Big One-Month Gain". 2 February 2017. http://www.water.ca.gov/news/newsreleases/2017/020217_snow_survey.pdf. Accessed 28 December 2017.

[70] California Department of Water Resources. "Snowpack's Water Content Remains Far above Average". 1 March 2017. http://www.water.ca.gov/news/newsreleases/2017/030117_snow_survey_release.pdf. Accessed 28 December 2017.

[71] State of California. Upper North Fork Feather River Hydroelectric Project, FERC #2105, Draft Environmental Impact Report. Chapter 3. California Environmental Protection Agency: State Water Resources Control Board. 2017. https://www.waterboards.ca.gov/waterrights/water_issues/programs/water_quality_cert/docs/upper_feather_ferc2105/eir2014nov/unffr_3.pdf. Accessed 28 December 2017.

[72] United States Geological Survey. "Feature Detail Report for: Lassen Peak." 19 January 2018. https://geonames.usgs.gov/apex/f?p=gnispq:3:0::NO::P3_FID:262324. Accessed 19 January 2018.

[73] California Department of Water Resources. "The State Water Project." 23 October 2012. http://www.water.ca.gov/state_water_project_home.cfm. Accessed 24 October 2017.

[74] B. Kerkez, S. D. Glaser, R. C. Bales, M. W. Meadows. Design and performance of a wireless sensor network for catchment-scale snow and soil moisture measurements. Water Resources Research, 48(9): W09515, 2012.

[75] B. Harrison, R. Bales. Skill Assessment of Water Supply Forecasts for Western Sierra Nevada Watersheds. Journal of Hydrologic Engineering, 21(4): 04016002, 2016.

[76] J. D. Miller, H. D. Safford, M. Crimmins, A. E. Thode. Quantitative Evidence for Increasing Forest Fire Severity in the Sierra Nevada and Southern Cascade Mountains, California and Nevada, USA. Ecosystems, 12: 16 – 32, 2009.

[77] A. L. Westerling, H. G. Hidalgo, D. R. Cayan, T. W. Swetman. Science, 313: 940 – 943, 2006.

[78] A. L. Westerling, B. P. Bryant. Climate change and wildfire in California. Climatic Change, 87(Suppl. 1): S231 – S249, 2008.

[79] E. C. Cordero, W. Kessomkiat, J. Abatzoglou, S. A. Mauget. The identification of distinct patterns in California temperature trends. Climatic Change, 108 (1 – 2): 357 – 382, 2011.

[80] M. L. Markstrom, L. E. Hay, M. P. Clark. Towards simplification of hydrologic modeling: identification of dominant processes. Hydrology and Earth System Sciences, 20: 4655–4671, 2016.

[81] N.S. Diffenbaugh, D. L. Swain, D. Touma. Anthropogenic warming has increased drought risk in California. Proceedings of the National Academy of Sciences, 1-6, 2015.

[82] F. Pianosi, T. Wagener. A simple and efficient method for global sensitivity analysis based on cumulative distribution functions. Environmental Modelling & Software, 67: 1-11, 2015.

[83] T. Wagener, N. McIntyre, M. J. Lees, H. S. Wheater, H. V. Gupta. Towards reduced uncertainty in conceptual rainfall-runoff modelling: dynamic identifiability analysis. Hydrological Processes, 17: 455 – 476, 2003.

[84] H. K. McMillan, E. Ö. Hreinsson, M. P. Clark, S. K. Singh, C. Zammit, M. J. Uddstrom. Operational hydrological data assimilation with the recursive ensemble Kalman filter. Hydrology and Earth System Sciences, 17: 21 – 38, 2013.

[85] S. A. Malek et al. Real-time Estimation of Spatial Snow Water Equivalent using Scarce In-situ Measurements and a Historical Product, in preparation.

APPENDIX A: Rain-on-Snow Study Methods

WSNs used in rain-on-snow analysis Figure A-1 shows the location of the considered WSNs over a satellite map of California. The outline of the three watersheds (Feather, American, and Kings) is included for context. Data was available for water years 2008-2016 in the Kings River; 2014-15 in the American; and 2017 in the Feather River.

Detecting rain-on-snow Rain-on-snow events were defined as any event in which, at some point during the event, at least 20mm of rain (0.78 inches) falls within 24 hours on at least 25cm of snow (9.84 inches). Partitioning between rain and snow was done using hourly data from co-located heated rain gauges and snow depth sensors. Rain gauges were assumed to measure total precipitation while snow depth sensors measure snowfall. Averages and ranges across sites and basins were calculated based on precipitation and snowfall data that were smoothed using a 24-hour moving average window. Snowfall events of intensity <5mm/hr (0.2 inches/hr) were discarded, as were temperatures at which the total recorded precipitation was less than 1% of total precipitation. Snow depth was converted to density using the method developed by [1].

Impact on rain-on-snow on snowpack SNOWPACK simulations at all sites in Figure A-1 were performed by enforcing snow depth to observed values (conditional assimilation in case of model underestimation based on simultaneous weather conditions, [6]). A canopy module was used to simulate different canopy features [23]. Canopy and soil parameters were estimated basing on satellite datasets, USDA SSURGO soil surveys, or literature values for sandy soils [57]. Leaf Area Index was adjusted node by node basing on satellite estimates (year 2017, see https://modis.gsfc.nasa.gov/data/dataprod/mod15.php) and observed snow depth during the year of maximum snow depth at each site. Liquid water flow in snow was simulated using Richards Equation [58], but a bucket-type approach was used in the Kings River as an approximation due to numerical instabilities in case of extremely dry soils [6].

Input data to the model include air temperature, relative humidity, wind speed, short- and long-wave radiation, and precipitation. Incoming long-wave radiation was internally estimated by the model. Solid precipitation was estimated from snow-depth sensors, whereas liquid precipitation was based on rain-gauge data, assuming a linear increase of rain proportion between 273.35 and 275.35 K.

Bucks Lake was excluded from simulations due to numerical instabilities, whereas Humbug data are not available for water year 2017. Data not available from wireless sensor networks were taken either from co-located weather stations or representative stations at similar elevation in the same basin (http://cdec.water.ca.gov/). Gaps in incoming shortwave radiation and wind speed were filled with the North American Land Data Assimilation System (NLDAS) datasets.

Impact of rain-on-snow on soil-water storage Soil-water storage is computed by depth-integrating measurements up to 60-cm depth at each site (1.96 ft). Rain-on-snow results include only events with at least 75% rain and average air temperature/relative humidity during periods of rain above -5 °C, and 80% respectively. The Feather River basin uses data from 36 sensor nodes, the Kings River basin uses data from 27 nodes.

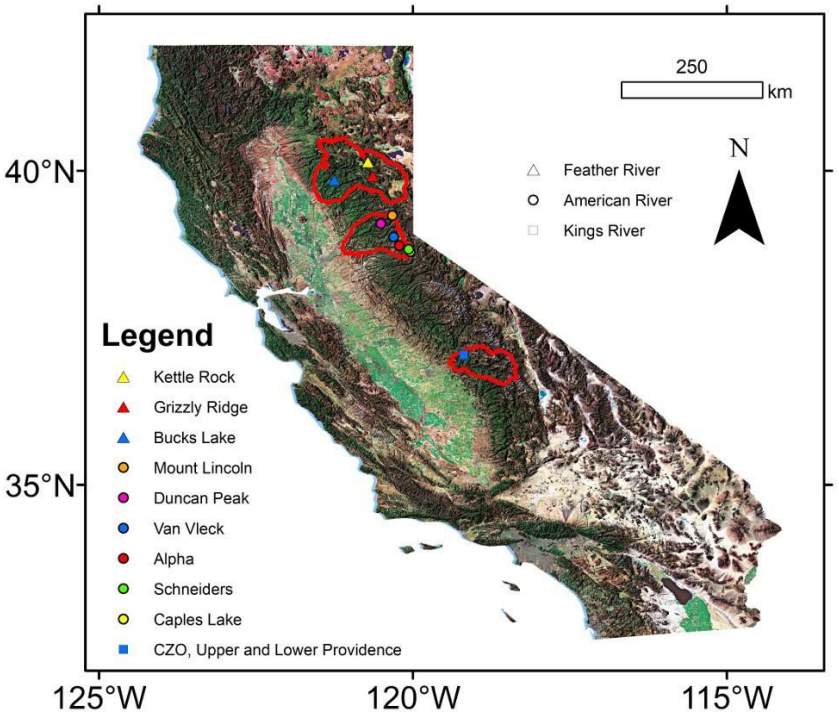

Figure A-1: Location of available wireless sensor networks across the Sierra Nevada and three different watersheds: Feather, American, and Kings River. 250 km corresponds to 155 miles.

APPENDIX B: Blended SWE Map Results

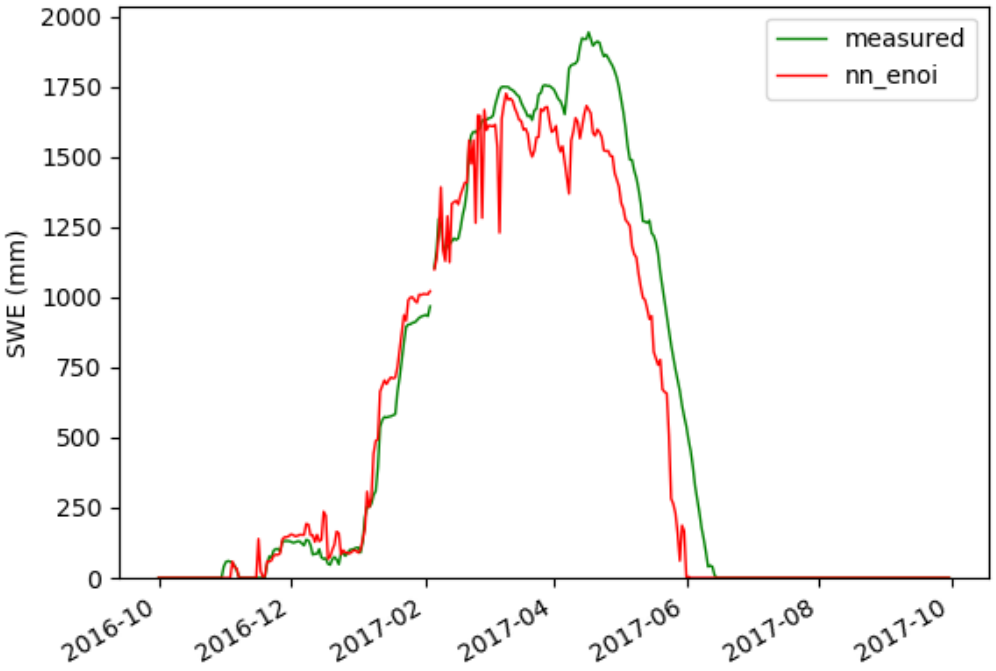

Figure B-1: Pilots Peak (PLP) snow pillow readings compared with NN-EnOI simulation. 1000 and 2000 mm correspond to 39.37 and 78.74 inches, respectively.

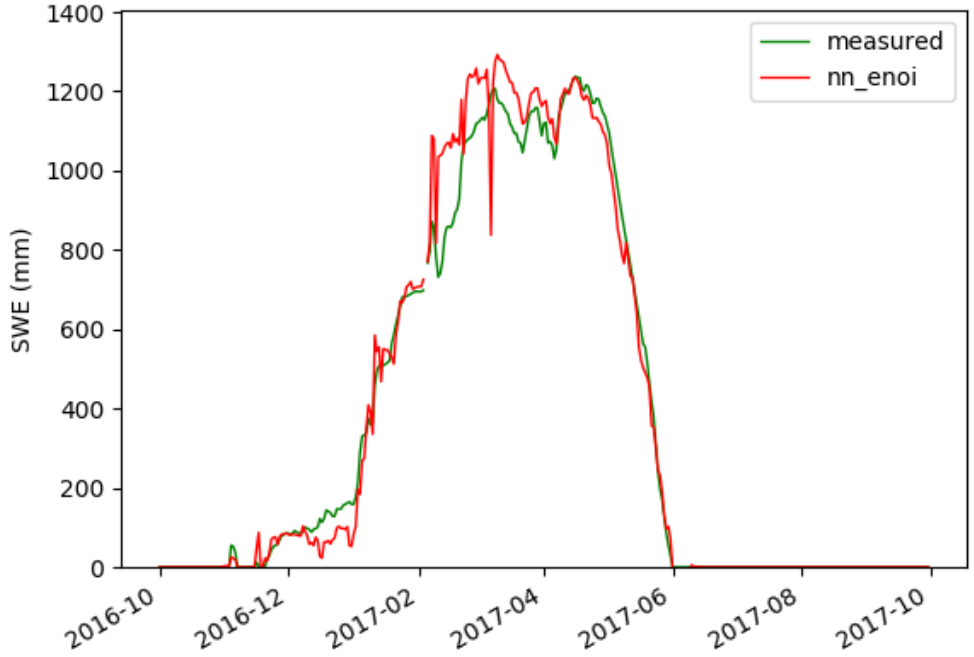

Figure B-2: Kettle Rock (KTL) snow pillow readings compared with NN-EnOI simulation (NN-EnOI stands for Nearest Neighbor - Ensemble Optimal Interpolation scheme). 600 and 1200 mm correspond to 23.6 and 47.24 inches, respectively.

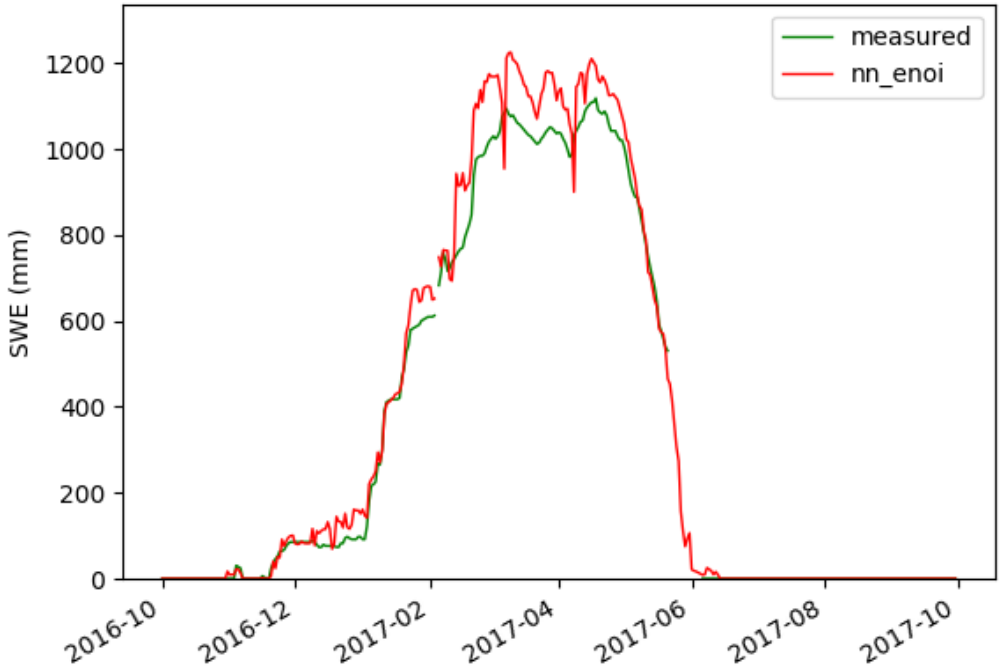

Figure B-3: Grizzly Ridge (GRZ) snow pillow readings compared with NN-EnOI simulation (NN-EnOI stands for Nearest Neighbor - Ensemble Optimal Interpolation scheme). 600 and 1200 mm correspond to 23.6 and 47.24 inches, respectively.

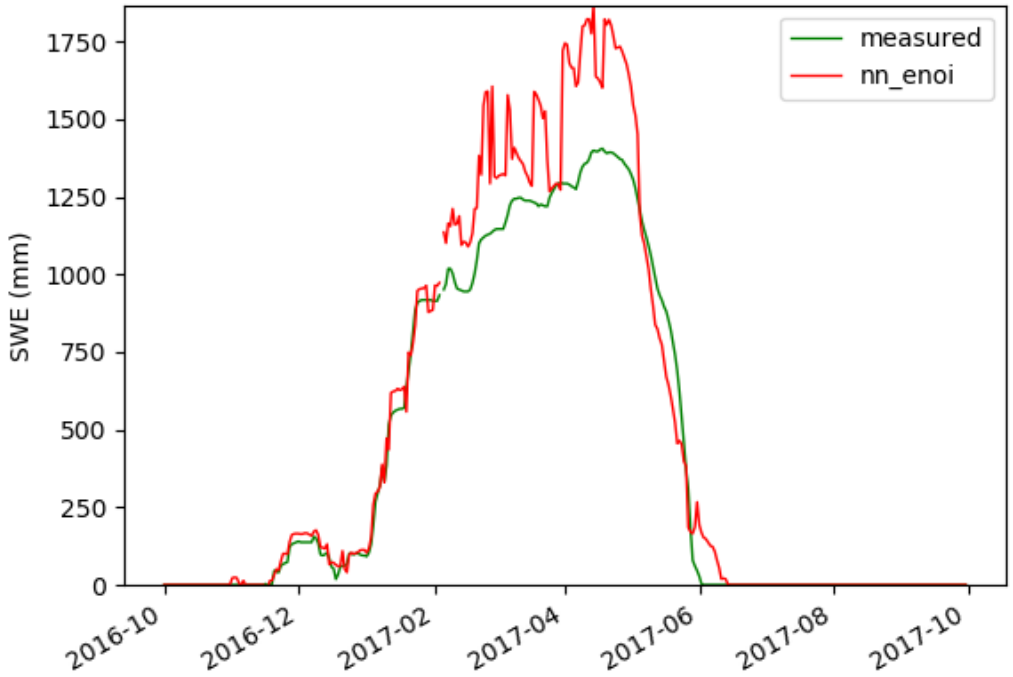

Figure B-4: Bucks Lake (BKL) snow pillow readings compared with NN-EnOI simulation (NN-EnOI stands for Nearest Neighbor - Ensemble Optimal Interpolation scheme). 750 and 1500 mm correspond to 29.53 and 59.05 inches, respectively.

APPENDIX C: Model Assessment and Recalibration Methods

Recalibration of the PRMS model is a multi-stage process. The first two steps (parameter sensitivity analysis and model uncertainty assessment) are being performed simultaneously. The most significant challenge with respect to the first step, parameter sensitivity, are the large (5000+) parameter spaces inherent to a distributed hydrologic model like PRMS as well as the nonlinearities present in such models. To address all parameters and avoid *a priori* assumptions about the relative importance of different parameters, we will start by using a grouped parameters method to reduce the number of parameters to a set that is independent and computationally feasible to analyze. Noninfluential parameters are then fixed to nominal values, while the most influential parameters will then be subjected to more rigorous sensitivity tests. We will perform our analysis using both variance- and density-based sensitivity methods to provide a robust parameter ranking before proceeding to model calibration. Both of these types of methods account for high-order parameter interactions, with density-based methods having the possible advantage of being moment independent, meaning they will characterize the entire parameter distribution better than variance-based methods in the case of highly skewed parameter sets [82].

The second of the first two steps, model uncertainty assessments, quantifies how well a model simulates a given process over a given period (and through which parameter values). Certain processes may be highly simplified in hydrologic models; for example, the Feather River PRMS model considers a two-layer snow module, where the profile of snow properties in not simulated [39]. Canopy-snow interactions are simulated with global, average parameters for both short-wave transmission through vegetation and canopy long-wave emission. Precipitation partitioning between rain and snow, meanwhile, is based on two static temperature thresholds, while soil-water storage dynamics rely on a conceptual separation between recharge zone, deeper soil moisture, and a subsurface reservoir [39]. Conversely, other processes may be well simulated by the model. By means of repeated performance evaluations with (stochastically) varying parameter values, uncertainty assessments distinguish time periods and/or processes that the model can simulate well, as opposed to those that cannot be properly simulated with any parameter combination [83]. This approach identifies the parameters (and assumptions) that are inadequate to simulate the process(es) they intend to and, by extension, the main source of predictive uncertainty in the model. Together with parameter sensitivity, this information is highly useful for model recalibration.

The USGS PRMS team recently performed a global sensitivity analysis for this model over the conterminous United States [80]. This analysis compared outcomes on a regional scale (for example, the Sierra Nevada versus the Appalachian Mountains versus the Great Plains), meaning that the range of processes involved was much broader than the dominant mechanisms driving streamflow on the Feather River. The 110,000 independent HRUs used by the USGS team were also much larger (between 5,400 ft^2 and 5,400 mi^2 or 500 m^2 and 14,000 km^2) than those used on the Feather River PRMS. However, the outcomes and methodological choices of this nation-wide assessment provide some useful guidelines for our work, for example regarding the parameters we may expect to emerge in first step of the sensitivity analysis.

Among the potential 108 parameter that PRMS uses (most of which potentially have different values for each HRU), the USGS PRMS team chose 35 parameters as an initial sensitivity pool. These parameters span all processes, from temperature and precipitation distribution to groundwater and runoff. The most sensitive parameters regarding snow melt (a key process on the Feather River), for example, resulted in being associated with precipitation distribution, radiation, and of course the snow module. Examples include *tmax_allsnow*, *tmax_allrain* (phase partitioning), *radmax* (radiation), *jh_coef* (evapotranspiration), and *freeh2o_cap* (liquid-water drainage threshold within the snow module [39]). While the USGS PRMS team did not consider temperature-distribution parameters, we expect temperature lapse rates to also play an important role in our recalibration on the Feather River.

The third step based on the results of the sensitivity analysis and model uncertainty is a global recalibration of the PRMS model. Model recalibration, even if undertaken with a reduced parameter set and across time periods that are optimal for parameter calibration, may still face challenges due to the nonlinear, nonconvex parameter spaces that are common in hydrologic models. Recalibration algorithms must be able to cover large areas of the parameter space, since parameter behavior may vary widely in different regions, and be robust to poor local minima. The chosen method for this step relies on existing USGS tools like LUCA [27], which uses a Shuffled Complex Evolution (SCE) algorithm [26]. SCE is a population-evolution algorithm, meaning it groups several potential solutions and evolves (i.e., moves) these groups towards local minima simultaneously. This grouping greatly improves the efficiency of the algorithm and allows it to search a large parameter space in a reasonable amount of time. Periodically, the evolution is paused and the potential solutions are shuffled and redistributed into new groups. This step allows information to be shared across groups and reduces the likelihood that a group of solutions will become trapped in poor local minima [18, 19]

The final step of the process is model validation (see Section 3.3.2). We plan to use a split-sample cross-validation technique, allowing us to leverage the WSN data for both model calibration and validation.